Biogeochemical Oceanographic Conditions on the Newfoundland and Labrador Shelf during 2021 and 2022

David Bélanger, Gary Maillet, Brittany Dalton, Alexandria Fudge, Devyn Ramsay, Shannah Rastin.

Science Branch
Newfoundland and Labrador Region
Environmental Sciences Division
Fisheries and Oceans Canada
Northwest Atlantic Fisheries Center
80, East White Hills Road
St. John's, NL
A1C 5X1

2025

Canadian Technical Report of Fisheries and Aquatic Sciences 3711

Fisheries and Oceans Canada | Pêches et Océans Canada

Canada

Canadian Technical Report of Fisheries and Aquatic Sciences

Technical reports contain scientific and technical information that contributes to existing knowledge but which is not normally appropriate for primary literature. Technical reports are directed primarily toward a worldwide audience and have an international distribution. No restriction is placed on subject matter and the series reflects the broad interests and policies of Fisheries and Oceans Canada, namely, fisheries and aquatic sciences.

Technical reports may be cited as full publications. The correct citation appears above the abstract of each report. Each report is abstracted in the data base *Aquatic Sciences and Fisheries Abstracts*.

Technical reports are produced regionally but are numbered nationally. Requests for individual reports will be filled by the issuing establishment listed on the front cover and title page.

Numbers 1-456 in this series were issued as Technical Reports of the Fisheries Research Board of Canada. Numbers 457-714 were issued as Department of the Environment, Fisheries and Marine Service, Research and Development Directorate Technical Reports. Numbers 715-924 were issued as Department of Fisheries and Environment, Fisheries and Marine Service Technical Reports. The current series name was changed with report number 925.

Rapport technique canadien des sciences halieutiques et aquatiques

Les rapports techniques contiennent des renseignements scientifiques et techniques qui constituent une contribution aux connaissances actuelles, mais qui ne sont pas normalement appropriés pour la publication dans un journal scientifique. Les rapports techniques sont destinés essentiellement à un public international et ils sont distribués à cet échelon. II n'y a aucune restriction quant au sujet; de fait, la série reflète la vaste gamme des intérêts et des politiques de Pêches et Océans Canada, c'est-à-dire les sciences halieutiques et aquatiques.

Les rapports techniques peuvent être cités comme des publications à part entière. Le titre exact figure au-dessus du résumé de chaque rapport. Les rapports techniques sont résumés dans la base de données *Résumés des sciences aquatiques et halieutiques.*

Les rapports techniques sont produits à l'échelon régional, mais numérotés à l'échelon national. Les demandes de rapports seront satisfaites par l'établissement auteur dont le nom figure sur la couverture et la page du titre.

Les numéros 1 à 456 de cette série ont été publiés à titre de Rapports techniques de l'Office des recherches sur les pêcheries du Canada. Les numéros 457 à 714 sont parus à titre de Rapports techniques de la Direction générale de la recherche et du développement, Service des pêches et de la mer, ministère de l'Environnement. Les numéros 715 à 924 ont été publiés à titre de Rapports techniques du Service des pêches et de la mer, ministère des Pêches et de l'Environnement. Le nom actuel de la série a été établi lors de la parution du numéro 925.

Canadian Technical Report
of Fisheries and Aquatic Sciences 3711

2025

Biogeochemical Oceanographic Conditions on the Newfoundland and Labrador Shelf during 2021 and 2022

[1]David Bélanger, [1]Gary Maillet, [1]Brittany Dalton, [1]Alexandria Fudge, [1]Devyn Ramsay, [1]Shannah Rastin.

Science Branch
Newfoundland and Labrador Region
Environmental Sciences Division
Fisheries and Oceans Canada
Northwest Atlantic Fisheries Center
80, East White Hills Road
St. John's, NL
A1C 5X1

Cat. No. Fs97-6/3711E-PDF ISBN 978-0-660-78137-2 ISSN 1488-5379

https://doi.org/10.60825/esn6-7677

Correct citation for this publication:

Bélanger, D., Maillet, G., Dalton, B., Fudge, A., Ramsay, D., and Rastin, S. 2025. Biogeochemical Oceanographic Conditions on the Newfoundland and Labrador Shelf during 2021 and 2022. Can. Tech. Rep. Fish. Aquat. Sci. 3711: ix + 34 p. https://doi.org/10.60825/esn6-7677

TABLE OF CONTENTS

LIST OF TABLES

LIST OF FIGURES

ABSTRACT

Bélanger, D., Maillet, G., Dalton, B., Fudge, A., Ramsay, D., and Rastin, S. 2025. Biogeochemical Oceanographic Conditions on the Newfoundland and Labrador Shelf during 2021 and 2022. Can. Tech. Rep. Fish. Aquat. Sci. 3711: ix + 34 p. https://doi.org/10.60825/esn6-7677

Biogeochemical data collected during AZMP seasonal surveys, along with satellite ocean colour observations for the Newfoundland and Labrador Shelf in 2021 and 2022, are presented and compared to long-term regional averages. Data interpretation was complicated by survey cancellations due to the COVID-19 pandemic and inconsistencies in survey timing between the two years. However, results highlighted the continuation of long-term trends in the region, including higher nutrient levels, as well as increasing zooplankton abundance and biomass since the mid-2010s. There was an overall decline in chlorophyll inventories (0-100 m) in 2021 and 2022 compared to previous years despite near or above-normal levels of deep nitrates (50-150 m), while phytoplankton blooms were, on average, earlier and longer than normal on the Newfoundland and Labrador shelves, contrasting with later and shorter-than-normal blooms on the Grand Banks. Mesozooplankton abundance, particularly copepods and non-copepods, along with total zooplankton biomass, were predominantly above normal in 2021, and near normal in 2022. Surface nitrate depletion at Station 27 during summer and fall 2021 and 2022, along with the limited vertical extent of chlorophyll *a* biomass during the spring bloom of 2022, were likely a consequence of the strong stratification of the water column on the Grand Bank during these two years.

RÉSUMÉ

Bélanger, D., Maillet, G., Dalton, B., Fudge, A., Ramsay, D., and Rastin, S. 2025. Biogeochemical Oceanographic Conditions on the Newfoundland and Labrador Shelf during 2021 and 2022. Can. Tech. Rep. Fish. Aquat. Sci. 3711: ix + 34 p.
https://doi.org/10.60825/esn6-7677

Les données biogéochimiques récoltées durant les relevés saisonniers, ainsi que les observations satellitaires de la couleur de l'océan pour la région de Terre-Neuve-et-Labrador en 2021 et 2022, sont présentées et comparées aux moyennes régionales à long-terme. L'interprétation des données a été compliquée par l'annulation de relevés due à la pandémie de COVID-19 et par les incohérences temporelles dans la réalisation des relevés entre les deux années. Cependant, les résultats ont mis en évidence une continuité dans les tendances à long-terme dans la région, notamment des niveaux plus élevés de nutriments ainsi qu'une hausse de l'abondance et de la biomasse du zooplancton depuis le milieu des années 2010. Dans l'ensemble, les inventaires de chlorophylle *a* (0-100 m) on déclinés en 2021 et 2022 en comparaison des années précédentes malgré des niveaux de nitrates en profondeurs (50-150 m) près, ou au-dessus de la normale, tandis que les floraisons printanières de phytoplancton ont été, en moyenne, plus hâtives et plus longues que la normale sur les plateaux de Terre-Neuve et du Labrador, contrastant avec des floraisons plus tardives et plus courtes que la normale sur les Grands Bancs. L'abondance du mésozooplancton, en particulier celle des copépodes et des non-copépodes, ainsi que la biomasse total du zooplancton, étaient principalement au-dessus de la normale en 2021, et près de la normale en 2022. Les concentrations particulièrement faibles de nitrates en surface à la Station 27 durant l'été et l'automne 2021 et 2022, ainsi que la répartition verticale limitée de la biomasse de chlorophylle *a* pendant la floraison printanière de 2022, étaient vraisemblablement dus à la forte stratification de la colonne d'eau sur les Grands Bancs durant ces deux années.

1. INTRODUCTION

The Atlantic Zone Monitoring Program (AZMP) was implemented in 1998 to bolster Fisheries and Oceans Canada's (DFO) capacity to describe, understand, and forecast the state of the marine ecosystem (Therriault et al. 1998). The AZMP gathers information on the marine environment and ecosystem from data collected at a network of sampling locations (high-frequency sampling stations, cross-shelf sections, and ecosystem trawl surveys) spread across four DFO regions (Québec, Gulf, Maritimes, and Newfoundland and Labrador), sampled at a frequency ranging from weekly to once-annually. The sampling design provides crucial information on the variability in physical and biogeochemical properties of the Northwest Atlantic continental shelf and slope waters on seasonal and inter-annual scales. Cross-shelf sections and ecosystem trawls surveys provide information about broad-scale environmental variability but are limited in their seasonal coverage. High-frequency sampling stations complement the broad-scale sampling by providing detailed information on seasonal changes in ocean properties. In addition to ship-based *in situ* observations, remote sensing of ocean colour measurements provides further insights into the distribution of phytoplankton in the ocean surface layer on a broad spatio-temporal scale.

The marine environment of the Newfoundland and Labrador (NL) Region is strongly influenced by the Labrador Current (LC). The inner branch of the LC transports cold and relatively fresher waters flowing from Baffin Bay through Davis Strait, and from Hudson Bay through Hudson Strait, over the continental shelf (Wang et al. 2015; Florindo-López et al. 2020). The stronger outer branch carries warmer, saltier and nutrient-rich waters along the continental slope into Flemish Pass, where it mixes with the warm and salty waters of the North Atlantic Current (Krauss et al. 1990; Townsend et al. 2004) (figure 1A). A density front at the shelf-break separates the cooler and fresher subarctic shelf waters from the warmer and saltier slope waters (Townsend et al. 2004). Another prominent feature of the NL shelf is the Cold Intermediate Layer (CIL), a cold water mass formed over the continental shelf during the spring when seasonal near-surface stratification isolates the cold winter mixed layer from the warmer atmosphere (Petrie et al. 1988; Cyr et al. 2011). The CIL is present during most of the year, maintaining bottom temperatures near 0°C. Other factors influencing NL water properties include sea ice, atmosphere-ocean heat exchange, precipitations, terrestrial runoffs, and wind mixing (Cyr et al. 2022, 2024).

Changes in the physical and biogeochemical environment influence both plankton community composition and annual biological production cycles, with implications for energy transfer to higher trophic levels. Understanding the seasonal production cycles of plankton and their variability on annual to decadal scales is essential for an ecosystem approach to fisheries management. This report aims to describe the biogeochemical environment in the Newfoundland-Labrador Shelves bioregion using a set of metrics to characterize important processes related to plankton production cycles and composition. These include surface and subsurface nutrient inventories, representing the availability of nutrients required for phytoplankton production, and surface layer chlorophyll *a* (chl *a*) inventories from *in situ* (0-100 m) and remote sensing (surface concentration) observations, representing phytoplankton biomass and spring bloom dynamics. Zooplankton metrics include total dry biomass and the abundance of copepods and non-copepods, reflecting the overall quantity of zooplankton present and the abundances of dominant taxa. Copepod relative abundance is used to assess general community composition along the main oceanographic sections, as well as seasonal variability at the high-frequency sampling site Station 27 (S27). Here, we present data primarily

averaged on monthly to annual scales and compare them to long-term average conditions in the region, with a focus on the years 2021 and 2022. This report also complements similar reviews of biogeochemical oceanographic conditions for the Scotian Shelf (Casault et al. 2023, 2024) and the Gulf of St. Lawrence (Blais et al. 2023a, 2023b).

2. METHODS

To the extent possible, sample collection and processing conform to established AZMP standard protocols described in Mitchell et al. (2002). Procedures for non-standard measurements or derived variables are described below. This report uses ecosystem production units (EPU) defined by the Northwest Atlantic Fisheries Organization (NAFO) (Koen-Alonso et al. 2019) to refer to the different subregions of the NL shelf and slope waters (figure 1B).

2.1 SATELLITE REMOTE SENSING OF OCEAN COLOUR

Near-surface chlorophyll *a* concentrations, a proxy for phytoplankton biomass, were estimated from satellite ocean colour imagery collected by the Moderate Resolution Imaging Spectroradiometer (MODIS) Aqua sensor.

We used the PhytoFit Shinny application (Clay et al. 2021) to compute metrics that characterize the phenology of the spring phytoplankton bloom for nine subregions (hereinafter referred to as polygons) spanning the NL shelf waters (figure 1B) as well as within a 50 km^2 polygon surrounding S27. For each year and polygon, the initiation, duration and magnitude of the spring bloom were calculated using a method adapted from Zhai et al. (2011). First, daily mean chl *a* concentrations were retrieved from remote sensing reflectance using the POLY4 regional band-ratio algorithm (Clay et al. 2019). Then, for each year, a loess regression, weighed according to spatial percent coverage, was fitted to the annual time series of daily mean chl *a* concentrations. Lastly, the fitted values of the loess regressions were used to model the spring bloom with a shifted Gaussian function of time from which the following bloom parameters were derived:

- Initiation = day of year (DOY) when chl *a* concentration increases to 20% of amplitude (i.e., maximum fitted value);
- Duration = number of days separating the initiation and the end (DOY when chl *a* concentration decreases to 20% of bloom amplitude);
- Magnitude = area under the Gaussian curve between the initiation and the end of the spring bloom and above chl *a* background level.

Bloom magnitude is a proxy for total net phytoplankton biomass production during the spring bloom. It does not account for biological processes such as grazing, sinking and/or lysis. Only days comprised within the period extending from the winter low chl *a* values to the lowest concentrations preceding the beginning of the fall bloom were used to model the spring bloom phenology.

2.2 SAMPLES COLLECTION

Seasonal oceanographic surveys are conducted in the spring, summer, and fall along standard cross-shelf sections in the NL Region. These surveys are complemented by occupations of S27 by ships of opportunity (figure 1B). Sampling involved vertical profiling of the water column using a rosette-mounted CTD (SBE-9plus, Sea-Bird Electronics) equipped with sensors for dissolved

oxygen, fluorescence, photosynthetically active radiation (PAR), pH, coloured dissolved organic matter (CDOM) and light attenuation (transmissometer). Water samples were collected in Niskin bottles at most stations and standard depths of 5, 10, 20, 30, 40, 50, 75, 100, 150, 250, 500, 1000 m, and near the bottom, depending on station bathymetry. All samples were analyzed for nutrients (nitrate, silicate and phosphate), while chl *a* concentration was measured down to a depth of 100 m along oceanographic sections and throughout the entire water column (175 m) at S27. Total alkalinity (TA) and dissolved inorganic carbon (DIC) were also measured at a subset of stations and depths, but the results are not presented here. Zooplankton samples were collected by vertically towing a conical ring net (75-cm diameter, 200-µm mesh) at a speed of approximately 1 $m \cdot s^{-1}$ from near bottom (or to a maximum depth of 1000 m) to the surface. Samples were preserved in a 2% buffered formaldehyde solution and analyzed for total biomass, abundance and diversity. Zooplankton individuals were identified at a taxonomic rank deemed appropriate for the program's objectives, with an emphasis on copepods.

2.3 VERTICALLY INTEGRATED VARIABLES

Integrated chl *a* (0-100 m) and nutrient inventories for the shallow (0-50 m) and deeper (50-150 m) layers were computed using trapezoidal numerical integration. The nearest near-surface measurements were used for surface (0 m) values. When the maximum depth at a given station was shallower than the lower depth limit of the integration interval, the lower integration depth corresponded to the station depth. If data at the lower integration limit were not available, the values were determined as follows: 1) by interpolation if sampling extended beyond he lower integration limit, or 2) by using the nearest deeper value if sampling was shallower than the lower integration limit.

2.4 ANNUAL ANOMALY SCORECARDS

Spatial and temporal trends of main biogeochemical indices are summarized in standardized anomaly scorecards. First, time series of vertically integrated nutrients, chl *a*, and zooplankton inventories were modeled with a linear model of the form:

$$Density = \alpha + \beta_{YEAR} + \delta_{STATION} + \gamma_{SEASON} + \varepsilon$$

for the oceanographic sections where *Density* is in units of $mmol \cdot m^{-2}$ (nutrients), $mg \cdot m^{-2}$ (chl *a*), $g \cdot m^{-2}$ (zooplankton biomass) or $individuals \cdot m^{-2}$ (zooplankton abundance), α is the intercept, ε is the error, and β, δ, and γ are the categorical effects of year, station, and season, respectively.

For S27 time series, the model was:

$$Density = \alpha + \beta_{YEAR} + \delta_{MONTH} + \varepsilon$$

where β and δ are the categorical effects of year and month, respectively. For both models, data were log-transformed (ln) to normalize the skewed distribution of the observations. In the case of zooplankton, the number one (1) is added to the density before transformation (ln [*Density* + 1]) to include observations where density equals zero. Model's least square means based on type III sums of squares were used as estimates of annual means. For each index, annual anomalies were calculated as the deviation of an individual year from the long-term mean of the reference periods or climatology: 2003-2020 for satellite ocean colour data, and 1999-2020 for nutrients, chl *a*, and zooplankton inventories. Anomalies are expressed as standardized quantities, i.e., by dividing each anomaly by the standard deviation of the climatological mean.

3. RESULTS

3.1 OCEANOGRAPHIC SAMPLING

In 2021, a total of 77 stations were occupied by the AZMP during the summer along standard oceanographic sections in addition to 8 occupations of S27 during AZMP surveys and by ships of opportunity. In 2022, 146 stations were occupied along the standard sections during the spring and fall surveys in addition to 29 occupations of S27 during the seasonal surveys and by ships of opportunity. The COVID-19 pandemic led to the cancellation of the Spring 2021 survey and a limited number of S27 occupations, particularly during the spring. Unforeseen issues related to the availability of science vessels resulted in the cancellation of the fall 2021 and summer 2022 AZMP surveys. More details on spatial and temporal coverage of the surveys are provided in table 1 and figure 2.

3.2 NUTRIENTS AND CHLOROPHYLL INVENTORIES

Primary production in the Northwest Atlantic (NWA) is primarily limited by the availability of nitrate, although silicate is also essential to the production of diatoms, which dominate the phytoplankton assemblage during spring and fall bloom events. Phosphate assumes greater importance during the summer when surface waters are largely depleted of nitrate and silicate and the phytoplankton assemblage is dominated by smaller flagellates and ciliates.

Primary production predominantly occurs in the well-lit upper portion of the water column. As a result, nutrient inventories in the surface layer typically exhibit greater variability, with significant drawdowns during periods of intense phytoplankton growth. In contrast, deeper nutrient inventories are more stable over time, as they are less influenced by biological processes. For this reason, deep nutrient inventories are considered more reliable indicators of oceanic primary production potential.

3.2.1 Oceanographic sections

Deep (50-150 m) inventories of nitrate and silicate exhibited similar long-term trends across the NL region, characterized by positive anomalies throughout most of the 2000s, followed by periods of primarily near-to-below-normal nitrate (2009-2014) and silicate (2012-2014) inventories (figure 3A, B). Deep phosphate inventories also displayed a general decrease during the early 2010s, with above-normal levels from 2000 to 2003, followed by periods of primarily near-normal (2004-2011) and below-normal (2012-2014) levels (figure 3C). Since 2015, deep nitrate, silicate and phosphate inventories have exhibited variability but have, on average, increased compared to the previous 3 to 5 years (figure 3A-C). Chl *a* biomass inventories (0-100) were predominantly near or above normal throughout the 2000s, declined to below-normal levels from 2011 to 2016 before returning to near-to-above-normal levels until 2020 (figure 3D).

Surface (0-50 m) inventories of nitrate and silicate were primarily above normal across the NL region during the early and mid-2000s, before declining to near-normal to below-normal levels from the late 2000s through the late 2010s, despite considerable variability (figure 4A, B). Surface phosphate inventories exhibited a slightly different variation pattern, with strong positive anomalies during the early 2000s, followed by a period of primarily near-normal to slightly-above-normal levels from 2004 to 2011, except for the below-normal levels observed across the region in 2005 and 2006 (figure 4C). Surface phosphates reached their lowest levels in 2012, with several record-low concentrations observed, and remained primarily near-to-below normal afterward, except for some above-normal observations during the mid-2010s (figure 4C).

In 2021, deep nitrate and silicate inventories exhibited variability, with above-normal levels observed on BB (nitrate) and FC (nitrate and silicate) sections, below-normal levels at S27 (nitrate) and on MB (silicate), and near-normal levels elsewhere (figure 3A, B). Deep phosphate inventories were near normal across the region (figure 3C). Shallow nitrate and phosphate inventories were near-to-below normal across the region compared to near or above-normal levels for silicate (figure 4A-C). Chl *a* inventories also displayed variability with near-normal levels observed on SI, FC, and at S27, and below-normal levels on MB and BB (figure 3D). The SEGB section was not occupied in 2021 for the first time since the beginning of the program in 1999.

In 2022, deep nitrate and silicate inventories were above normal across the Newfoundland Shelf and the Grand Bank, including record-high nitrate levels on BB and at S27, while phosphate inventories were below normal on SI, and near-normal elsewhere (figure 3A-C). Surface nitrate, silicate and phosphate inventories showed similar patterns, with mainly below-normal levels on the Newfoundland Shelf, including record-low levels for all three nutrients on SI, near-normal levels at S27 and on FC, and above-normal levels on SEGB (figure 4A, B and C). Integrated chl *a* inventories were above normal on the Newfoundland Shelf and below normal across the Grand Banks (figure 3D). The MB section on the Labrador Shelf was not occupied in 2022 for the first time since 2016.

3.2.2 Station 27

The vertical distribution of nitrate, silicate, and phosphate exhibit similar seasonal patterns characterized by strong vertical concentration gradients known as nutriclines. During spring, rising air temperature induces water column stratification which, combined with longer daylight hours, trigger the onset of the phytoplankton bloom. The rapid uptake of nutrients by the growing phytoplankton biomass leads to the formation of nutriclines that persist throughout the summer. In the fall, cooling air temperatures and stronger winds gradually break down water column stratification, allowing for the replenishment of surface nutrient stocks through vertical mixing with deeper, nutrient-rich waters (figure 5A-C).

Nutrient climatologies at S27 indicate that nitrate, silicate and phosphate are relatively evenly distributed across most of the water column from January through March (figure 5A-C). Significant nutrient drawdowns are observed in April, with nutrient concentrations in surface waters remaining low from May through November before gradually increasing again in December (figure 5A-C). Conversely, nutrients in near-bottom waters generally follow an opposite seasonal pattern, with concentrations increasing from April through November and declining from December through March (figure 5A-C).

In 2021, field work limitations associated with the COVID epidemic hindered data collection at S27 until June. Furthermore, no water samples were collected in September and October. Surface nitrate inventories experienced important depletion from June through November (figure 5A). Silicate and phosphate concentrations were also below average during the summer months in the top 50 m of the water column (figure 5B, C). The lack of data for the first five months of the year prevented the characterization of the chl *a* vertical distribution profile during the spring. Chl *a* concentration was low in June and July, but above-average levels between 50 and 100 m in August suggested the development of a late-summer subsurface chlorophyll maximum at mid-water depths (figure 5D).

In 2022, nitrate inventories experienced significant depletion from May through November in the upper 40 m of the water column (figure 5A). Silicate concentrations in the upper water column were slightly lower than average from May through August while surface phosphate was lowest

in September-October, approximately two months later than the average timing (figure 5B, C). Bottom concentrations of nitrate and silicate at depths greater than 120 m were higher than usual starting from April on, except for September, when the relatively uniform vertical distribution of nutrients indicated deep vertical mixing of the water column caused by Hurricane Fiona (figure 5A, B). The high chl *a* concentration observed during the spring was constrained to the top 50-60 m of the water column and was below average at greater depths (figure 5D). Chl *a* decreased below average levels during the summer months, then increased in September across the top 50 m of the water column, remaining above average through the fall (figure 5D).

3.3 PHYTOPLANKTON BLOOM PHENOLOGY

3.3.1 Satellite polygons

The initiation of the spring phytoplankton bloom shifted from generally later than normal from 2014 to 2017 to mainly near or earlier than normal across the region since 2018 (figure 6A). In 2021, the timing of the spring bloom displayed a latitudinal pattern with earlier-than-normal onsets in central Labrador and on the Newfoundland shelf, near normal onsets on the northern Grand Bank and in the Flemish Pass, and later-than-normal onsets on the southern Grand Bank and southern Newfoundland (figure 6A). Spring bloom timing in 2022 also exhibited a latitudinal pattern but with later onsets compared to 2021 from the central Newfoundland Shelf (St. Anthony Basin) to the south. Bloom initiation timing was earlier than normal in Central Labrador and on the northern Newfoundland Shelf (Hamilton Bank) for a third consecutive year, near-normal on the central and southern Newfoundland Shelf, and later than normal across the Grand Bank and The Flemish Pass/Cap for the first time since 2017 (figure 6A).

The shift to earlier spring bloom observed around 2018 was associated with longer bloom duration on the Newfoundland and Labrador shelves, but this was not the case on the Flemish Pass/Cap, the Grand Bank, and in Southern Newfoundland, where bloom duration has remained mainly shorter than normal since 2020 (figure 6B). In 2021, bloom duration was near normal in Central Labrador and on the northern Newfoundland Shelf, longer than normal on the central and southern Newfoundland Shelf and on the Flemish Cap, and shorter than normal in the Flemish Pass, on the Grand Bank and in Southern Newfoundland (figure 6B). In 2022, bloom duration was longer than normal in Central Labrador, near normal on the Newfoundland Shelf and on the Flemish Pass/Cap, and shorter than normal on the Grand Bank and in Southern Newfoundland for a second consecutive year (figure 6B).

Bloom magnitude varied substantially between 2003 and 2011 but has remained mostly near or below normal since 2012, besides some localized positive anomalies and the above-normal levels observed from the central Newfoundland Shelf to the Northern Grand Bank and the Flemish Pass/Cap in 2018 and 2019 (figure 6C). Spring bloom magnitude in 2021 and 2022 showed a similar pattern, with near to below normal levels across the region, except for the positive anomalies observed on the Flemish Cap and the St. Pierre Bank in 2021 and 2022, respectively (figure 6C).

3.3.2 Station 27

Satellite observations at S27 indicate that surface chl *a* concentration typically begins increasing in March, peaks around mid-April, and then declines to a summer minimum in early June, remaining low until late July (figure 7A). Chl *a* starts increasing again in August, reaching a fall maximum in late October, before declining again from November through March (figure 7A). Satellite data are generally not available from December to early January.

In 2021, satellite observations indicated that surface chl *a* concentrations were near average from January to mid-May and above average in late May and early June, extending the duration

of the bloom beyond the normal period (figure 7A, B). Bloom initiation occurred earlier than normal, and magnitude was slightly lower than normal (figure 7B). However, limited satellite coverage from late March to late April introduced uncertainty to these model-derived indices.

In 2022, surface chl *a* concentrations were above average during the winter and peaked around mid-April, as it typically does, but at higher-than-normal levels (figure 7A). Ship-based observations confirmed elevated chl *a* concentrations during the spring bloom but also showed that phytoplankton biomass was confined to the top 50 m of the water column, with below-average concentrations at greater depths (figure 5D). Surface chl *a* then declined to below-average levels in early May, resulting in a shorter-than-normal duration of the bloom (figure 7A, B). As in 2021, limited satellite coverage during the early phase of the bloom introduced uncertainty regarding the model-derived late timing and near normal magnitude (figure 7B).

3.4 ZOOPLANKTON DIVERSITY, BIOMASS AND ABUNDANCE

3.4.1 Oceanographic sections

Community composition

The mesozooplanton community in the NWA is predominantly composed of copepods, both in terms of abundance and biomass. The eight most abundant copepods species/taxa in the study area account for approximately 90% of total copepod abundance and can be categorized into two groups based on body size (figure 8A). Large copepods, including three *Calanus* species (*C. finmarchicus*, *C. glacialis*, and *C. hyperboreus*), are not numerically dominant but are primary contributors to total zooplankton biomass. Zooplankton abundance on the other hand is primarily driven by small copepod taxa, particularly the widely distributed *Pseudocalanus* spp. and *Oithona* spp., which collectively account for more than half of the total copepod population (figure 8A). *Temora longicornis* may also significantly contribute to the total copepod abundance on the Grand Bank (FC and SEGB; figure 8A).

The non-copepods fraction of the community typically comprises 30-40% of total zooplankton abundance. Appendicularians (pelagic tunicates), pteropods (pelagic gastropods), ostracods and cladocerans typically account for more than half of total non-copepods individuals, while bivalve and echinoderm meroplanktonic larvae may also be abundant (figure 8B). Malacostraca includes organisms such as decapods (shrimps), euphausiids (krill), amphipods, mysids and isopods which are normally associated with the macrozooplankton size fraction, i.e., larger than 20 mm.

Abundance and biomass

Total zooplankton biomass was lowest during the initial 2-3 years of the program and had generally remained primarily near or above normal since then with the exception of a period of near-to-below normal levels from 2012 to 2015 (figure 9A). Interannual variations in zooplankton biomass generally reflect fluctuations in the abundance of the three large *Calanus* copepod species , particularly *Calanus finmarchicus* (figure 9A-D). Total copepods abundance on the Newfoundland and Labrador shelves (MB, SI and BB) has been variable since 1999, but exhibited a more gradual increase on the Grand Bank (FC, SEGB; figure 10A). Since 2015, total copepod abundance, along with the abundance of numerically dominant *Oithona* spp. and *Pseudocalanus* spp. copepods, have remained predominantly near or above normal across the region (figure 10A-C). Non-copepod abundance followed a similar pattern to total copepods exhibiting greater variability on the Newfoundland and Labrador shelves and shifting from

predominantly below-normal to mainly above-normal on the Grand Bank around the mid-2010s (figures 10A and 11A).

In 2021, zooplankton biomass and total copepod abundance were above normal across all sampled sections, with record-high biomasses observed on SI and BB (figures 9A and 10A). Above-normal abundances of *C. finmarchicus*, *C. glacialis* and *C. hyperboreus* on SI and BB contributed to the record-high biomass levels on the Newfoundland Shelf (figure 9A-D). The abundance of numerically dominant small *Oithona* spp., *Pseudocalanus* spp., and *T. longicornis* were either near or above normal with record-high levels of *Pseudocalanus* spp. on BB, and *T. longicornis* on SI (figure 10B-D). Total copepod abundance was above normal on MB and SI despite near-normal abundances of two of the three most dominant small copepod taxa, suggesting above-average contributions from typically less abundant species such as *C. finmarchicus* (figures 9B and 10A-D). The abundance of non-copepods including appendicularians and pteropods, were near-to-above-normal across the region, continuing trends that started in 2015 for total non-copepods, and 2016 for appendicularians (figure 11). Record-high levels were observed on FC for pteropods and total non-copepods (on par with 2016; figure 11A, C).

In 2022, zooplankton biomass was normal on all sections except for SI where the above-normal level by record-high abundances of *C. glacialis* and *C. hyperboreus* (figure 9A, C and D). Total copepod abundance was normal on the Newfoundland Shelf (SI and BB) and above normal on the Grand Bank (FC and SEGB), reflecting the abundance pattern of *Oithona* spp. (figure 10 A, B). The abundance of *Pseudocalanus* spp. was primarily above normal, with a record high level on SI, while *T. longicornis* exhibited more variability (figure 10C, D). Non-copepod abundance, including appendicularians and pteropods, were near or above normal across the region, with a record-high abundance of pteropods on SEGB, on par with 2020 (figure 11).

3.4.2 Station 27

Community composition

Copepod community composition at S27 reflects that observed along the main AZMP sections, especially for the northern Grand Bank (FC), with the three *Calanu*s species and small *Oithona* spp., *Pseudocalanus* spp. and *T. longicornis* taxa accounting for approximately 90% of total copepod abundance (figure 12A). *Oithona* spp. and *Pseudocalanus* spp. dominate the abundance year-round, whereas *T. longicornis* becomes abundant only during late summer and fall (August-December). The abundance of *C. finmarchicus* typically peaks in June and gradually declines throughout the rest of the year, while the presence of the larger and more Arctic *C. glacialis* and *C. hyperboreus* is mainly restricted to spring and summer (April-July) (figure 12A).

The non-copepod community is numerically dominated by appendicularians (e.g., *Frittilaria* spp., *Oikopleura* spp.) and pteropods (e.g., *Limacina helicina, Limacina retroversa*) year-round with appendicularians typically accounting for more than half of total non-copepods from April through July, and pteropods being most abundant from September through May (figure 12B). Pelagic bivalve larvae are also abundant from August through January while cladocerans only occur in significant number from July through October (figure 12B).

In 2021, S27 was occupied only once monthly from April through September, in addition to one and two occupations in November and December, respectively. Therefore, seasonal variations in zooplankton community composition for that year are based on snapshot observations rather

than average conditions. The copepod community structure departed from the climatology mainly by lower spring (May-June) proportions of *C. glacialis* and *C. hyperboreus* and a high proportion of *T. longicornis* in late summer (August-September). For non-copepods, the proportions of cladocerans in August and of bivalve larvae in September, were approximately two times higher than climatology (figure 12D).

In 2022, the copepod community structure departed from the climatology mainly by the reduced proportion of *C. finmarchicus* in August and September, and of *T. longicornis* in August, October and November (figure 12E). For the non-copepods, the main differences from the climatology were the high proportion of pteropods in March of and the lower-than normal proportion of bivalve larvae in August (figure 12F).

Abundance and biomass

Zooplankton biomass shows a maximum value in April and a second, more modest, peak in June (figure 13A). During the spring phytoplankton bloom, zooplankton tows performed with 200-µm mesh net also collect, in addition to zooplankton, substantial amounts of large chain-forming diatoms. The April biomass peak is therefore partly driven by the presence of phytoplankton in the samples. The June biomass peak, on the other hand, coincides with maximum abundances of the three large *Calanus* species known to contribute the most to total zooplankton biomass (figure 13A-C). Total copepod abundance at S27 is highest from September through January, a period during which the numerically dominating copepods *Pseudocalanus* spp., *Oithona* spp. and *T. longicornis* are most abundant (figure 14). Declining zooplankton biomass during that period highlights the comparatively limited impact of small copepod taxa on total biomass (figures 13A and 14). The abundance non-copepod peaks in May and September at the time of maximum abundance of appendicularians and pteropods, respectively (figure 15). A second peak in appendicularian abundance occurs in July when pteropod abundance is minimum (figure 15B, C). The bimodal distribution in appendicularians likely reflects the multispecies aspect of that taxonomic grouping.

In 2021, zooplankton biomass exhibited temporal variability. The above-normal biomass observed in May and the below-normal biomass in September reflected the abundance pattern of *C. finmarchicus* (figure 13A, B). In contrast, the June below-normal biomass was likely driven by below-normal abundances of *C. glacialis* and *C. hyperboreus* (figures 13A, C and D). Total copepod abundance also fluctuated, primarily driven by the two most abundant taxa, *Pseudocalanus* spp. and *Oithona* spp. (figures 14A-C). Non-copepod abundance was near-normal from April through July, with an above-normal spike in May (figure 15A). It then decreased to slightly below-normal levels from August to mid-November before increasing to near-to-above-normal levels in late November and December (figure 15A). Both appendicularians and pteropods exhibited markedly high abundances in early December (figure 15B, C).

In 2022, zooplankton biomass was mainly near-to-below-normal during the spring and fall months, with a few notably high values observed in in September (figure 13). In two instances, the above-normal biomass in September was seemingly driven by unusually high abundances of small *Oithona* spp., *Pseudocalanus* spp., *T. longicornis* copepods and non-copepods, rather than by large *Calanus* copepods (figures 13, 14 and 15). The seasonal abundance pattern for total non-copepods reflected, for the most part, those of numerically dominant appendicularians and/or pteropods (figures 15). However, other non-copepod taxa such as cladocerans were

apparently responsible for the unusually high non-copepod abundance observed in early September (figures 12F and 15).

Population dynamics of key copepod species

C. finmarchicus copepods have an annual life cycle characterized by a succession of five copepodite stages leading to sexual maturity. Pre-adults (CV) emerge from diapause – an overwintering period spent at depth – in the spring to spawn after molting into adults (CVI). The newly produced generation then develops into CI-CV stages throughout the spring and summer, dominating the population structure during this time (figure 16A). By fall, most individuals have reached the pre-adult CV stage and have accumulated energy reserves in preparation for diapause (figure 16A).

In 2021, the lower proportion of adults (CVI) and higher proportion of CI-CIII in April-May compared to the climatology suggested earlier-than-normal spawning of *C. finmarchicus* (figure 16B). However, the lack of sampling prior to April prevents us from confirming that this was associated with earlier emergence and molting of CV pre-adults into adults in late winter and early spring. The increased proportion of adults in August, followed by rising proportions of CI-CIII stages in September, also suggests the production of a second cohort in late summer (figure 16B). In 2022, the proportion of adult *C. finmarchicus* presumably peaked in March (no data for the January-February period), compared to April for the climatology, suggesting early sexual maturation of CV pre-adults (figure 16C). Similarly to 2021, the high proportion of young CI-CIII stages observed in September and October was indicative of a second cohort (figure 16C).

The *Pseudocalanus* spp. population in the Northwest Atlantic comprises several species with overlapping ranges and remarkably similar morphology (Aarbakke et al. 2014). Because of constraints associated with species identification, *Pseudocalanus* copepods are herein treated as multispecies complex. Differences in reproduction timing and number of generations have been reported both between species and among individuals (McLaren et al. 1989). However, population dynamics based on long-term observations at S27 suggests that dominant *Pseudocalanus* species typically exhibit an annual life cycle characterized by the production of a single generation (figure 16D).

In 2021, the *Pseudocalanus* spp. population dynamics, was characterized by a higher proportion of young CI-CIII stages in April compared to the climatology, suggesting an early spawning or faster development of the newly produced generation (figure 16E). The absence of sampling from January through March, however, makes it impossible to characterize the population structure during that period. In 2022, the proportion of adults potentially peaked in March (no sampling conducted prior to that), approximately one month earlier than normal (figure 16F). When compared to the climatology, the proportion of young CI-CIII stages peaked in May instead June, while that of CIV and CV stages peaked in August instead of September (figure 16F), indicating an early production cycle similar to what was observed in 2021. However, contrary to *C. finmarchicus*, the population dynamics of *Pseudocalanus* spp. did not show evidence of muti-generation production in 2021 or 2022 (figure 16E, F).

4. DISCUSSION

The increase in deep nutrient inventories across the NL Region in 2015-2016 was followed by an increase in chl *a* inventories. However, chl *a* biomass decreased to below-normal levels in 2021 on the Newfoundland and Labrador shelves, and in 2022 on the Grand Bank for the first

time since 2017. The relatively low chl *a* inventories of 2021 could be partly explained by the seasonal sampling being restricted to the summer, when chl *a* concentration are typically lowest. However, chl *a* inventories on MB, a section only sampled during the summer, were also below normal. Additionally, satellite observations showed that the magnitude of the spring bloom was near-to-below normal throughout most of the region. The absence of AZMP sampling in spring and fall 2021 makes it difficult to interpret the nutrient and chl *a* variation patterns and their relationships to the physical environment, especially given the variability in the results. However, the generally earlier and longer spring blooms on the Newfoundland and Labrador shelves suggest that the onset of water column stratification, which is one of the factors triggering the initiation of the spring bloom, occurred relatively early in these areas. In contrast, on the Grand Bank, the spring blooms were shorter, with a near or later-than-normal timing.

In situ observation for 2022 showed corresponding patterns between nutrients, chl *a*, and physical environmental conditions. The below-normal chl *a* levels on the Grand Bank contrasted with the conditions on the above-normal levels of Newfoundland Shelf (BB and SI). Similar to 2021, satellite observations showed early timing and normal to above-normal spring bloom duration for the Newfoundland and Labrador Shelf, in contrast to later and shorter-than-normal blooms on the Grand Bank. High sea surface temperatures and low surface salinity resulted in stronger-than-normal spring water column stratification at S27 in 2022 (Cyr et al. 2024). These conditions are generally associated with an early timing of the spring bloom (Ji et al. 2008; Cyr et al. 2023); therefore, it is unclear what caused the delayed initiation of the bloom across the Grand Bank. Other environmental factors, such as low light levels and copepod grazing, could delay the spring bloom initiation after the onset of stratification (Bautista and Harris 1992; Jardine et al. 2021).

Although no samples were collected at S27 during the spring of 2021, summer observations indicated severe nitrate depletion and lower-than-average chl *a* biomass during that period. In 2022, high surface nitrate concentrations in March fueled spring primary production at S27, resulting in high chl *a* biomass in April. However, stronger-than-normal stratification likely confined phytoplankton production to the top 50-60 m of the water column during the spring bloom (Cyr et al. 2024). The NL region was affected by Hurricane Fiona in late September of 2022. The large waves and strong winds associated with this severe weather event momentarily disrupted the stratification of the water column, allowing for vertical mixing with deeper nutrient-rich water. This nutrient input into surface waters improved fall bloom conditions, resulting in above-average chl *a* biomass, as captured by in situ and satellite observations at S27, and potentially on a larger scale in the NL region.

Both copepod abundance and zooplankton biomass were primarily above normal across the NL region for a second consecutive year in 2021. Seasonal sampling in 2021 was limited to summer, when the abundance of large *Calanus* spp. copepods – a major driver of zooplankton biomass – is at its maximum, which may have inflated the biomass values on the Grand Bank (FC) and the Newfoundland Shelf (BB and SI). However, both copepod abundance and zooplankton biomass were above normal on MB, a section sampled exclusively in summer, suggesting that the high abundance and biomass levels observed in 2021 were not solely an artifact of the truncated sampling season. Above-normal abundance of *C. finmarchicus*, a key contributor to zooplankton biomass, during year with early spring bloom timing has been consistently observed in the NL Region since the start of the monitoring program (Cyr et al. 2023). This phenomenon is believed to be linked to reduced cannibalistic predation pressure

from adult females on the newly produced generation during a shorter pre-bloom period, when phytoplankton biomass remains low (Bonnet et al. 2004; Plourde et al. 2009).

The limited number and temporal coverage of observations at S27 did not reveal major deviations from normal zooplankton biomass and abundance conditions in 2021. The population structure of *C. finmarchicus* suggests good recruitment of young copepodite stages in March, with the potential production of a second generation in September. However, the lack of data in October and the rapid decline in the proportion of CI-CIII stage by November introduces uncertainty. The production of multiple *C. finmarchicus* generations in subarctic waters has been linked to warmer sea temperatures, which are associated with earlier spawning and/or accelerated development of the first generation given adequate food supply (Head et al. 2013; Weydmann et al. 2018).

Copepod abundance and zooplankton biomass both declined in 2022 compared to the previous year. The abundance of large *Calanus* copepods is typically highest during the summer. Therefore, the absence of a summer survey in 2022 may partly explain the decline in *Calanus* abundance and zooplankton biomass indices. On the other hand, delayed spring bloom onsets were observed on most of the Newfoundland Shelf and the Grand Banks in 2022 which may have impacted *C. finmarchicus* recruitment due to increased predation pressure during this extended pre-bloom period of low phytoplankton biomass (Bonnet et al. 2004; Plourde et al. 2009). Conversely, the above-normal chl *a* concentration and early timing of the bloom on the northern Newfoundland Shelf (SI section and Hamilton Bank polygon) may have favored *C. glacialis* and *C. hyperboreus* recruitment and contributed to the above-normal zooplankton biomass in that area.

Abnormally high zooplankton biomass and abundances of both copepods and non-copepods at Station 27 in September 2022 suggest that zooplankton production benefited from the surge of the fall phytoplankton biomass associated with the passage of Hurricane Fiona. The population structure of *C. finmarchicus* at S27 shows evidence of the production of a second generation in September-October. There was no evidence of a second generation of *Pseudocalanus* spp. copepods, so the high September abundances were likely due to higher spawning success and/or survival of individuals from the first generation. However, both abundance and biomass declined to near-to-below normal levels by October-November indicating a short-lived positive impact of Hurricane Fiona on secondary production.

5. CONCLUSION

The assessment of biogeochemical conditions in the Canadian Northwest Atlantic for 2021 and 2022 was hindered by limitations and inconsistencies in the AZMP seasonal surveys conducted during these years. Despite these challenges, the findings reflect the continuation of long-term trends in the region, including an overall increase in nutrient and chlorophyll *a* concentrations, along with increases in zooplankton abundance and biomass since the mid-2010s. However, higher-resolution observations at S27 suggest that the strong stratification of the water column, driven by the unusually high surface temperature and low salinity (Cyr et al. 2024), may inhibit vertical mixing, potentially reducing the duration and vertical extent of phytoplankton production during the spring bloom.

Additionally, elevated water temperatures have been linked to shifts in the phytoplankton community composition, favoring a higher proportion of smaller-sized cells (Sommer and

Lengfellner 2008), and promoting multiple generation of key zooplankton species such as *Calanus finmarchicus* (Head et al. 2013; Weydmann et al. 2018) with potential impacts on the size structure of the planktonic community. Recent observations suggest improved productivity at the lower trophic level; however, the long-term effects of ocean warming on plankton community composition and phenological processes remain uncertain. Consistent seasonal monitoring of biogeochemical conditions by the AZMP is critical to understanding how ongoing climate change will affect the health and productivity of Canada's marine ecosystems.

6. SUMMARY

- Annual estimates of the keys indices for the sections were based on summer observations only in 2021, and on spring and fall observations in 2022 due to the cancellation of the spring and fall 2021 and 2022 cross-shelf surveys increasing uncertainty of the annual estimates.

2021

- Chlorophyll *a* inventories were near to below normal, following a period of near to above normal levels since 2017.
- Spring bloom initiation was earlier than normal on the Newfoundland and the Labrador shelves with the earliest bloom on record for the St. Anthony Basin.
- Total zooplankton biomass was above normal on all sections, including record-high biomass levels across the Newfoundland Shelf (SI and BB).
- Total copepod abundance was above normal on all section including record-high abundances of *Calanus finmarchicus* and *Temora longicornis* on FC, and *Pseudocalanus* spp. on BB.

2022

- Sub-surface (50-150 m) nitrate and silicate inventories were primarily above normal across the region including record-high nitrate levels on BB and at Station 27.
- The abundance of *C. glacialis and C. hyperboreus* copepods was at record-high levels on SI.
- The seasonal production cycle of *C. finmarchicus* copepods at S27 showed evidence of a second cohort in the fall.

7. ACKNOWLEDGEMENTS

The authors thank the personnel at the North Atlantic Fisheries Center who contributed to sample collection, sample analysis, data analysis, data management, and data sharing. We also thank the officers and crews of the Canadian Coast Guard Ships *Teleost, Vladykov, Alfred Needler, John Cabot*, *Capt. Jacques Cartier,* and the British RRS *James Cook* and American RV *Atlantis,* for their assistance in the collection of oceanographic data during 2021 and 2022. Reviews by Benoit Casault and Marjolaine Blais have improved the manuscript.

REFERENCES

Aarbakke, O.N.S., Bucklin, A., Halsband, C., and Norrbin, F. 2014. Comparative phylogeography and demographic history of five sibling species of *Pseudocalanus* (Copepoda: Calanoida) in the North Atlantic Ocean. J. Exp. Mar. Bio. Ecol. **461**: 479–488. doi:https://doi.org/10.1016/j.jembe.2014.10.006.

Bautista, B., and Harris, R.P. 1992. Copepod gut contents, ingestion rates and grazing impact on phytoplankton in relation to size structure of zooplankton and phytoplankton during a spring bloom. Mar. Ecol. Prog. Ser. **82**(1): 41–50. Inter-Research Science Center. Available from http://www.jstor.org/stable/24827422.

Blais, M., Galbraith, P.S., Plourde, S., and Lehoux, C. 2023a. Chemical and Biological Oceanographic Conditions in the Estuary and Gulf of St. Lawrence during 2022. Can. Tech. Rep. Hydrogr. Ocean Sci. 357 v + 70 p.

Blais, M., Galbraith, P.S., Plourde, S., Lehoux, C., and Devine, L. 2023b. Chemical and Biological Oceanographic Conditions in the Estuary and Gulf of St. Lawrence during 2021. DFO Can. Sci. Advis. Sec. Res. Doc. 2023/045. iv + 74 p.

Bonnet, D., Titelman, J., and Harris, R. 2004. *Calanus* the cannibal. J. Plankton Res. **26**(8): 937–948. doi:10.1093/plankt/fbh087.

Casault, B., Beazley, L., Johnson, C., Devred, E., and Head, E. 2024. Chemical and biological oceanographic conditions on the Scotian Shelf and in the eastern Gulf of Maine during 2022. Can. Tech. Rep. Fish. Aquat. Sci. 3589 vi + 72 p.

Casault, B., Johnson, C., Devred, E., Head, E., and Beazley, L. 2023. Optical, Chemical, and Biological Oceanographic Conditions on the Scotian Shelf and in the eastern Gulf of Maine during 2021. DFO Can. Sci. Advis. Sec. Res. Doc. 2023/016. v + 74 p.

Clay, S., Layton, C., and Devred, E. 2021. BIO-RSG/PhytoFit: First release (v1.0.0). Zenodo. https://doi.org/10.5281/zenodo.4770754.

Clay, S., Peña, A., DeTracey, B., and Devred, E. 2019. Evaluation of satellite-based algorithms to retrieve chlorophyll-*a* concentration in the Canadian Atlantic and Pacific Oceans. Remote Sens. **11**(22): 1–29. doi:10.3390/rs11222609.

Cyr, F., Bourgault, D., and Galbraith, P.S. 2011. Interior versus boundary mixing of a cold intermediate layer. J. Geophys. Res. Ocean. **116**(12): 1–12. doi:10.1029/2011JC007359.

Cyr, F., Coyne, J., Snook, S., Bishop, C., Galbraith, P.S., Chen, N., and Han, G. 2024. Physical Oceanographic Conditions on the Newfoundland and Labrador Shelf during 2022. Can. Tech. Rep. Hydrogr. Ocean Sci. 377 iv + 53 p.

Cyr, F., Lewis, K., Bélanger, D., Regular, P., Clay, S., and Devred, E. 2023. Physical controls and ecological implications of the timing of the spring phytoplankton bloom on the Newfoundland and Labrador shelf. Limnol. Oceanogr. Lett. **9**(3): 191–198. Available from https://doi.org/10.1002/lol2.10347 [accessed 28 August 2024].

Cyr, F., Snook, S., Bishop, C., Galbraith, P.S., Chen, N., and Han, G. 2022. Physical Oceanographic Conditions on the Newfoundland and Labrador Shelf during 2021. DFO Can. Sci. Advis. Sec. Res. Doc. 2022/040. iv + 48 p.

Florindo-López, C., Bacon, S., Aksenov, Y., Chafik, L., Colbourne, E., and Penny Holliday, N.

2020. Arctic Ocean and Hudson Bay freshwater exports: New estimates from seven decades of hydrographic surveys on the Labrador shelf. J. Clim. **33**(20): 8849–8868. doi:10.1175/JCLI-D-19-0083.1.

Head, E.J.H., Melle, W., Pepin, P., Bagøien, E., and Broms, C. 2013. On the ecology of *Calanus finmarchicus* in the Subarctic North Atlantic: A comparison of population dynamics and environmental conditions in areas of the Labrador Sea-Labrador/Newfoundland Shelf and Norwegian Sea Atlantic and Coastal Waters. Prog. Oceanogr. **114**: 46–63. Elsevier Ltd. doi:10.1016/j.pocean.2013.05.004.

Jardine, J.E., Palmer, M., Mahaffey, C., Holt, J., Wakelin, S., and Artioli, Y. 2021. Climatic controls on the spring phytoplankton growing season in a temperate shelf sea. J. Geophys. Res. Ocean. **127**(e2021JC017209). Available from https://doi.org/10.1029/2021JC017209.

Ji, R., Davis, C.S., Chen, C., Townsend, D.W., Mountain, D.G., and Beardsley, R.C. 2008. Modeling the influence of low-salinity water inflow on winter-spring phytoplankton dynamics in the Nova cotian Shelf-Gulf of Maine region. J. Plankton Res. **3430**(12): 1399–1416. doi:10.1029/2007GL032010.

Koen-Alonso, M., Pepin, P., Fogarty, M.J., Kenny, A., and Kenchington, E. 2019. The Northwest Atlantic Fisheries Organization Roadmap for the development and implementation of an Ecosystem Approach to Fisheries: structure, state of development, and challenges. Mar. Policy **100**: 342–352. Elsevier Ltd. doi:10.1016/j.marpol.2018.11.025.

Krauss, W., KäSe, R.H., and Hinrichsen, H.-H. 1990. The branching of the Gulf Stream southeast of the Grand Banks. J. Geophys. Res. **95**(C8): 13089–13561. doi:10.1029/jc095ic08p13089.

McLaren, I.A., Laberge, E., Corkett, C.J., and Sévigny, J.-M. 1989. Life cycles of four species of *Pseudocalanus* in Nova Scotia. Can. J. Zool. **67**(3): 552–558. NRC Research Press. doi:10.1139/z89-078.

Mitchell, M., Harrison, G., Pauley, K., Gagné, K., Maillet, G., and Strain, P. 2002. Atlantic Zonal Monitoring Program Sampling Protocol. Can. Tech. Rep. Hydrogr. Ocean Sci. 223 iv + 23 pp.

Petrie, B., Akenhead, B., Lazier, J., and Loder, J. 1988. The cold intermediate layer on the Labrador and Northeast Newfoundland shelves, 1978-1986. NAFO Sci. Coun. Stud. **12**: 57–69.

Plourde, S., Maps, F., and Joly, P. 2009. Mortality and survival in early stages control recruitment in *Calanus finmarchicus*. J. Plankton Res. **31**(4): 371–388. doi:10.1093/plankt/fbn126.

Sommer, U., and Lengfellner, K. 2008. Climate change and the timing, magnitude, and composition of the phytoplankton spring bloom. Glob. Chang. Biol. **14**(6): 1199–1208. doi:10.1111/j.1365-2486.2008.01571.x.

Therriault, J.-C., Petrie, B., Pepin, P., Gagnon, J., Gregory, D., Helbig, J., Herman, A., Lefaivre, D., Mitchell, M., Pelchat, B., Runge, J., and Sameoto, D. 1998. Proposal for a northwest Atlantic zonal monitoring program. Can. Tech. Rep. Hydrogr. Ocean Sci. 194: vii+57 p.

Townsend, D.W., Thomas, A.C., Mayer, L.M., Thomas, M., and Quinlan, J. 2004. Oceanography of the northwest Atlantic continental shelf. Sea Glob. Coast. Ocean Interdiscip. Reg. Stud. Synth. (June): 119–168. Available from

http://wavy.umeoce.maine.edu/pdf/2005_TheSea_Townsendetal_Chapt5.pdf.

Wang, Z., Yashayaev, I., and Greenan, B. 2015. Seasonality of the inshore Labrador current over the Newfoundland shelf. Cont. Shelf Res. **100**: 1–10. Elsevier. doi:10.1016/j.csr.2015.03.010.

Weydmann, A., Walczowski, W., Carstensen, J., and Kwasniewski, S. 2018. Warming of subarctic waters accelerates development of a key marine zooplankton *Calanus finmarchicus*. Glob. Chang. Biol. **24**: 172–183. Available from https://doi.org/10.1111/gcb.13864.

Zhai, L., Platt, T., Tang, C., Sathyendranath, S., and Hernández Walls, R. 2011. Phytoplankton phenology on the Scotian Shelf. ICES J. Mar. Sci. **68**(4): 781–791. doi:10.1093/icesjms/fsq175.

TABLES

Table 1. Summary table of the number of CTD casts, Niskin water samples and zooplankton samples collected in 2021 and 2022 at Station 27 (S27) and along oceanographic sections Southeastern Grand Bank (SEGB), Flemish Cap (FC), Bonavista Bay (BB), Seal island (SI) and Makkovik Bank (MB) during AZMP seasonal surveys and by ships of opportunity (SOO). See figure 1 for location of Station 27 and oceanographic sections.

Date	Survey	Section	CTD	Water (sampling depth in meters)														Zooplankton
				5	10	20	30	40	50	75	100	150	250	500	1000	Btm	Total	
2021																		
29 Jun - 19 Jul	AZMP summer	S27	2	2	2	2	2	2	2	2	2	2	0	0	0	7	25	4
		FC	33	24	23	24	22	24	24	22	21	16	6	3	2	16	227	24
		BB	15	13	13	13	10	13	13	13	13	10	8	4	3	12	138	13
		SI	15	11	11	11	10	11	11	10	10	8	4	3	1	9	110	10
		MB	12	12	12	12	10	12	12	12	11	10	4	2	2	11	122	12
23 Apr - 20 Dec	SOO	S27	8	3	3	3	2	3	3	3	3	3	0	0	0	3	29	7
2022																		
10 Apr - 1 May	AZMP spring	S27	5	5	5	5	5	5	5	5	5	5	0	0	0	5	50	5
		SEGB	22	16	16	16	16	16	15	8	7	7	5	4	4	16	146	16
		FC	35	25	25	25	25	24	25	25	22	15	6	4	4	20	245	25
		BB	15	14	14	14	14	14	14	14	14	13	8	5	4	13	155	14
22 Oct - 8 Nov	AZMP fall	S27	4	4	4	4	4	4	4	4	4	4	0	0	0	4	40	4
		SEGB	18	15	15	15	15	15	15	7	6	6	4	3	3	14	133	15
		FC	24	24	24	24	24	23	24	25	21	15	6	3	3	19	235	24
		BB	12	12	14	14	14	14	14	14	13	13	7	4	3	14	150	13
		SI	11	11	11	11	11	11	11	10	9	9	3	2	2	11	112	11
10 Jan - 30 Nov	SOO	S27	27	12	13	13	12	13	13	13	12	11	0	0	0	13	125	29

FIGURES

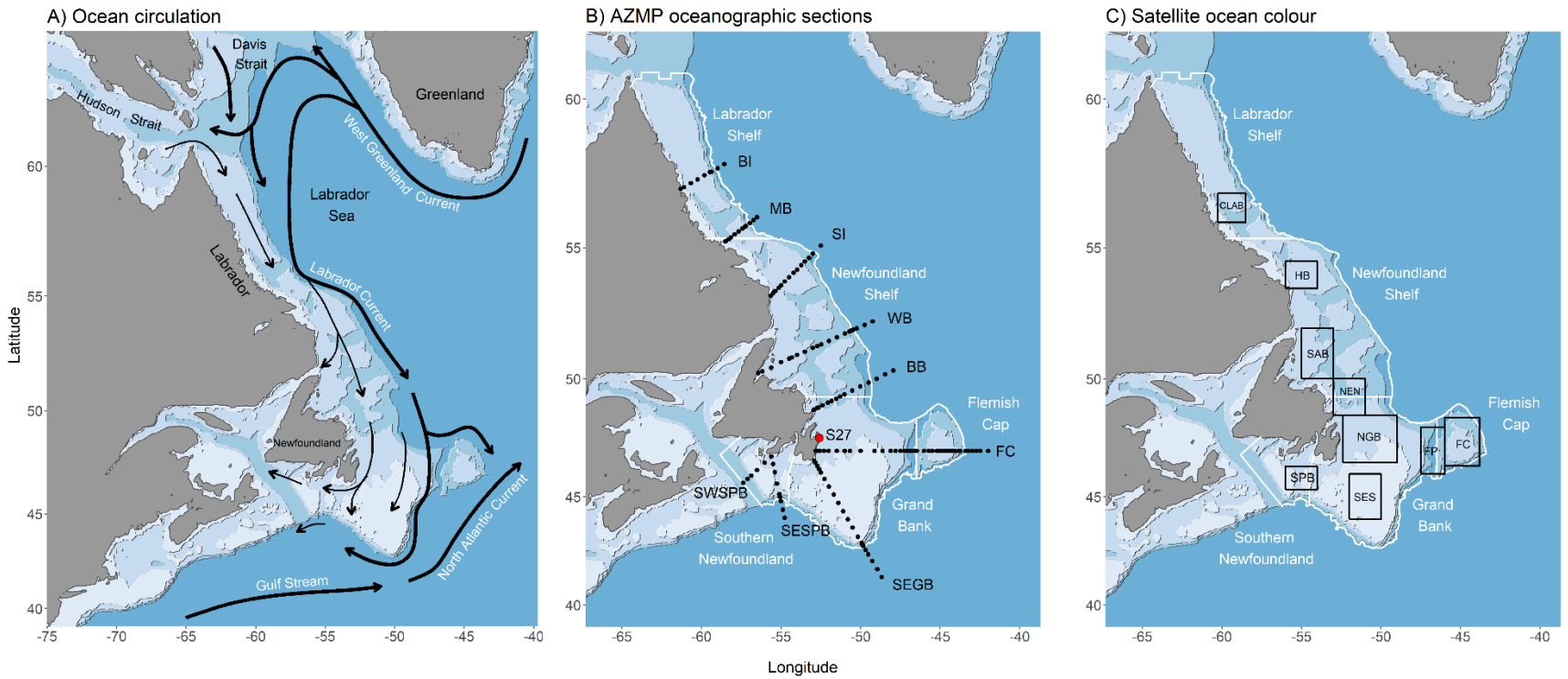

Figure 1. A) Ocean circulation in the Newfoundland and Labrador Region. B) Location of AZMP standard oceanographic sections (BI=Beachy Island, MB=Makkovik Bank, SI=Seal Island, WB=White Bay, BB=Bonavista Bay, FC=Flemish Cap, SEGB=Southeast Grand Bank, SWSPB=Southwest St. Pierre Bank, SESPB=Southeast St. Pierre Bank) and high-frequency monitoring station (S27) occupied by the AZMP since 1999 in the Newfoundland and Labrador Region. Black dots represent sampling stations along each section. C) Polygons used to calculate spring phytoplankton bloom indices (initiation, duration and magnitude) using satellite ocean colour data (CLAB=Central Labrador, HB=Hamilton Bank, SAB=St. Anthony Basin, NEN=Northeast Newfoundland, NGB=Northern Grand Bank, FP=Flemish Pass, FC=Flemish Cap, SES=Southeast Shoal, SPB=St. Pierre Bank). NAFO's Ecosystem Production Units (EPUs) used in this report to refer to the different subregions of the Newfoundland and Labrador Shelf are indicated in white in panels B and C.

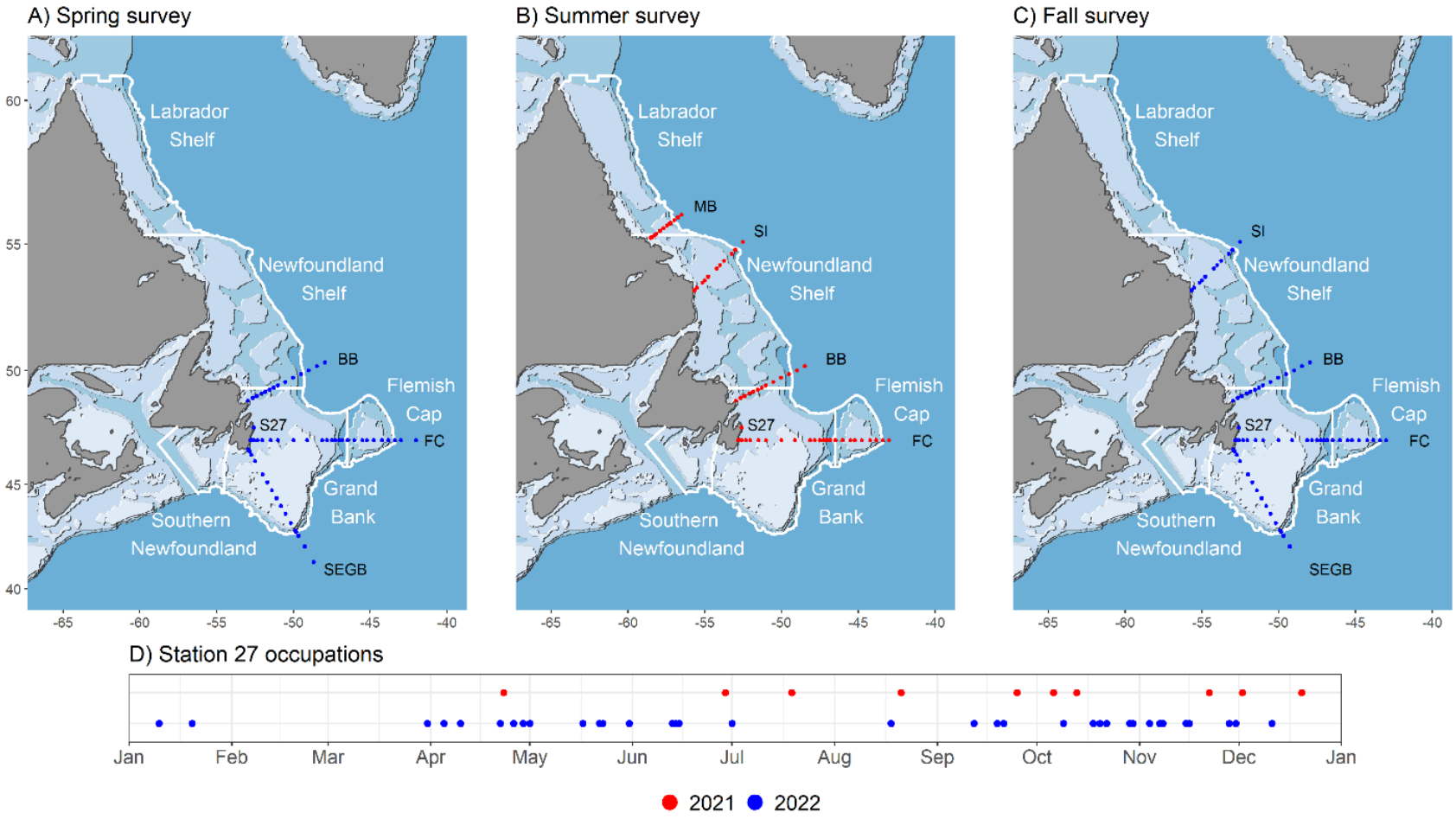

Figure 2. Summary of stations occupied during the 2021 and 2022 (A) the spring, (B) summer, and (C) fall AZMP surveys as well as (D) the number and time oy year of S27 occupations by AZMP and ships of opportunity. See Table 1 for AZMP survey dates.

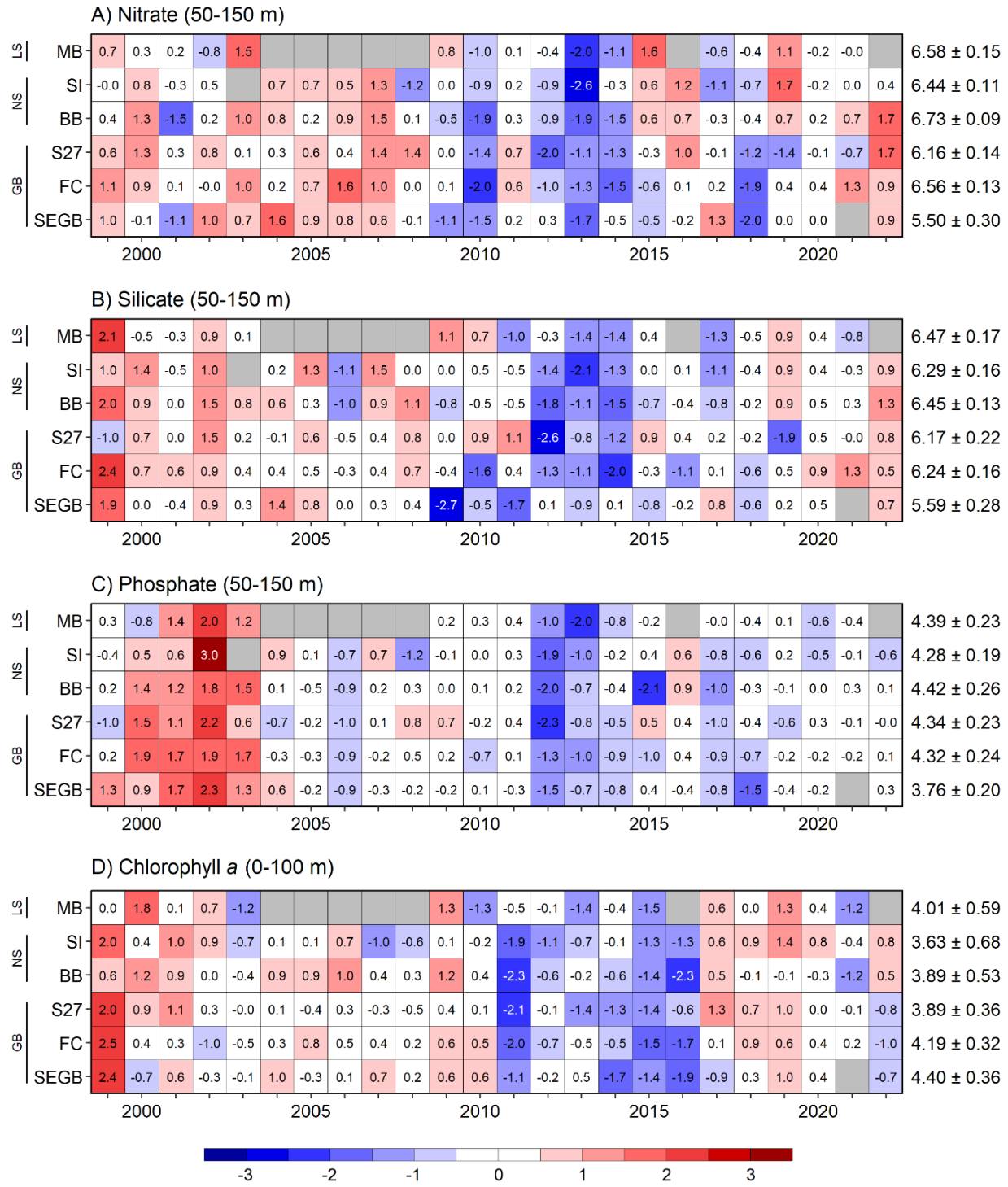

Figure 3. Scorecards of annual anomalies for deep inventories of (A) nitrate, (B) silicate, and (C) phosphate, as well as for (D) surface chlorophyll a (chl a). Numbers in the cells represent standardized anomalies based on a 1999-2020 climatology. Climatological means and standard deviations (SD) are listed to the right in units of ln(1 + concentration in mmol·m^{-2}) for nutrients, and of ln(concentration in mg·m^{-2}) for chl a. White cells indicate near-normal concentrations (±0.5 SD relative to the climatological mean), while blue/red cells indicate lower/higher-than-normal concentrations. Grey cells represent missing data. AZMP sections are listed from north (top) to south (bottom) on the left and grouped by subregions (EPUs): LS=Labrador Shelf, NS=Newfoundland Shelf, GB=Grand Bank. See Figure 1B for locations of AZMP sections and EPUs.

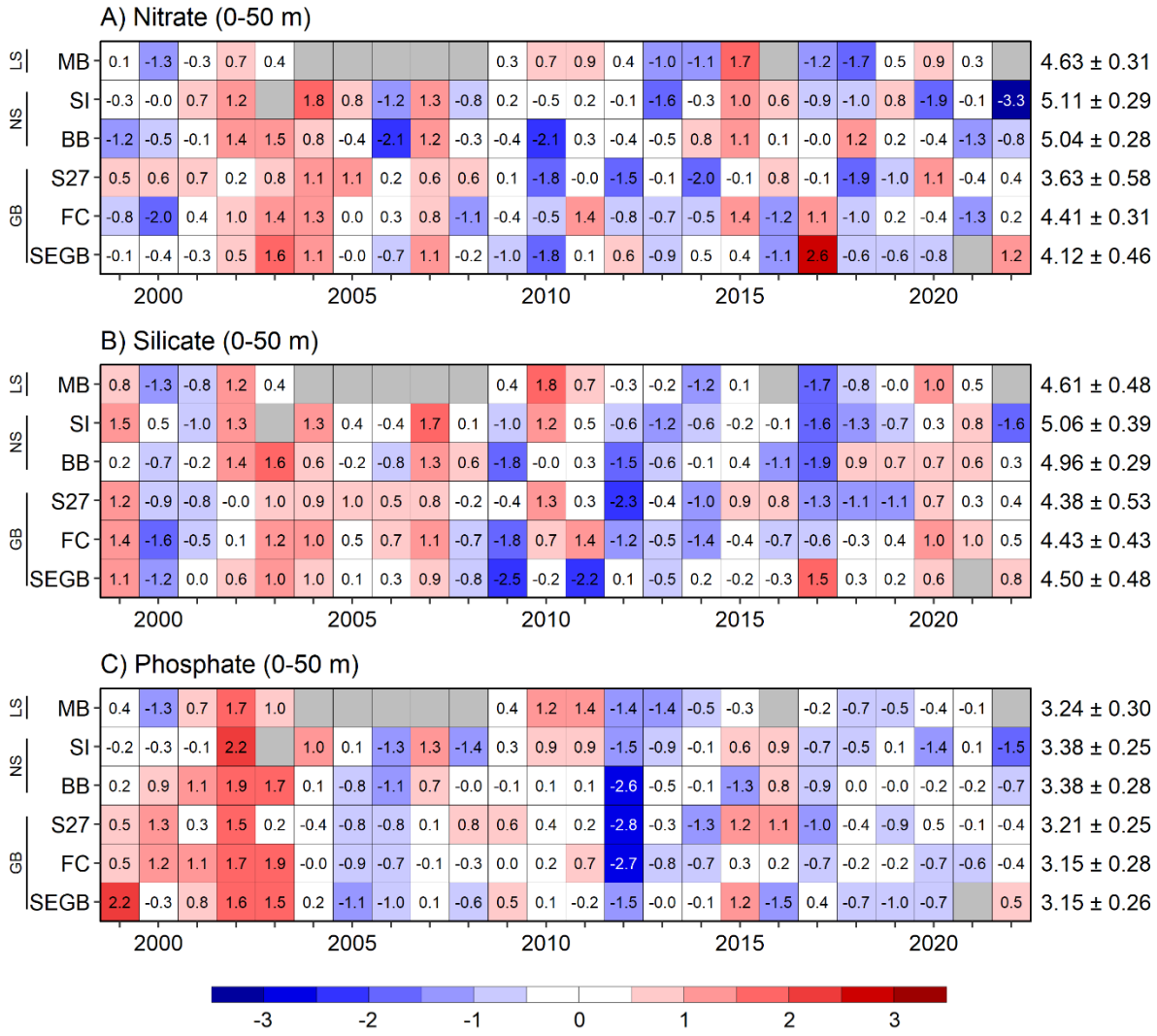

Figure 4. Scorecards of annual anomalies for surface inventories of (A) nitrate, (B) silicate, and (C) phosphate. Numbers in the cells represent standardized anomalies based on a 1999-2020 climatology. Climatological means and standard deviations (SD) are listed to the right in units of ln(1 + concentration in mmol·m^{-2}). White cells indicate near-normal concentrations (±0.5 SD relative to the climatological mean), while blue/red cells indicate lower/higher-than-normal concentrations. Grey cells represent missing data. AZMP sections are listed from north (top) to south (bottom) on the left and grouped by subregions (EPUs): LS=Labrador Shelf, NS=Newfoundland Shelf, GB=Grand Bank. See Figure 1B for locations of AZMP sections and EPUs.

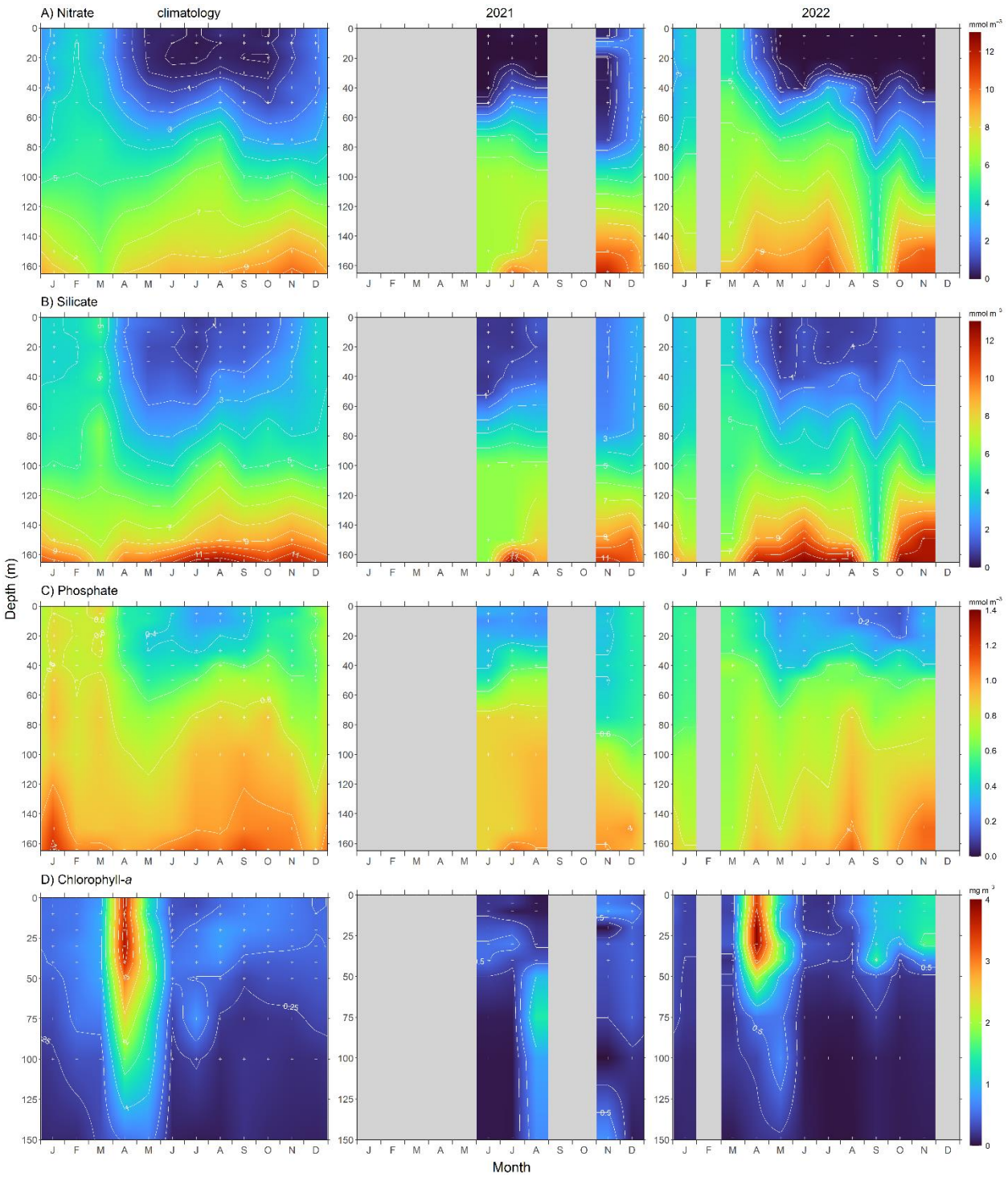

Figure 5. Seasonal variation in the vertical distribution of (A-C) nutrients and (D) chlorophyll a measured from water samples collected at Station 27. Climatologies represent average conditions during the 1999-2020 reference period. Data were averaged by collection depth and month, then interpolated using a 10-depth by 12-month grid (white crosses; see section 2.2 for details on water collection methodology). Grey areas represent periods during which no data were available.

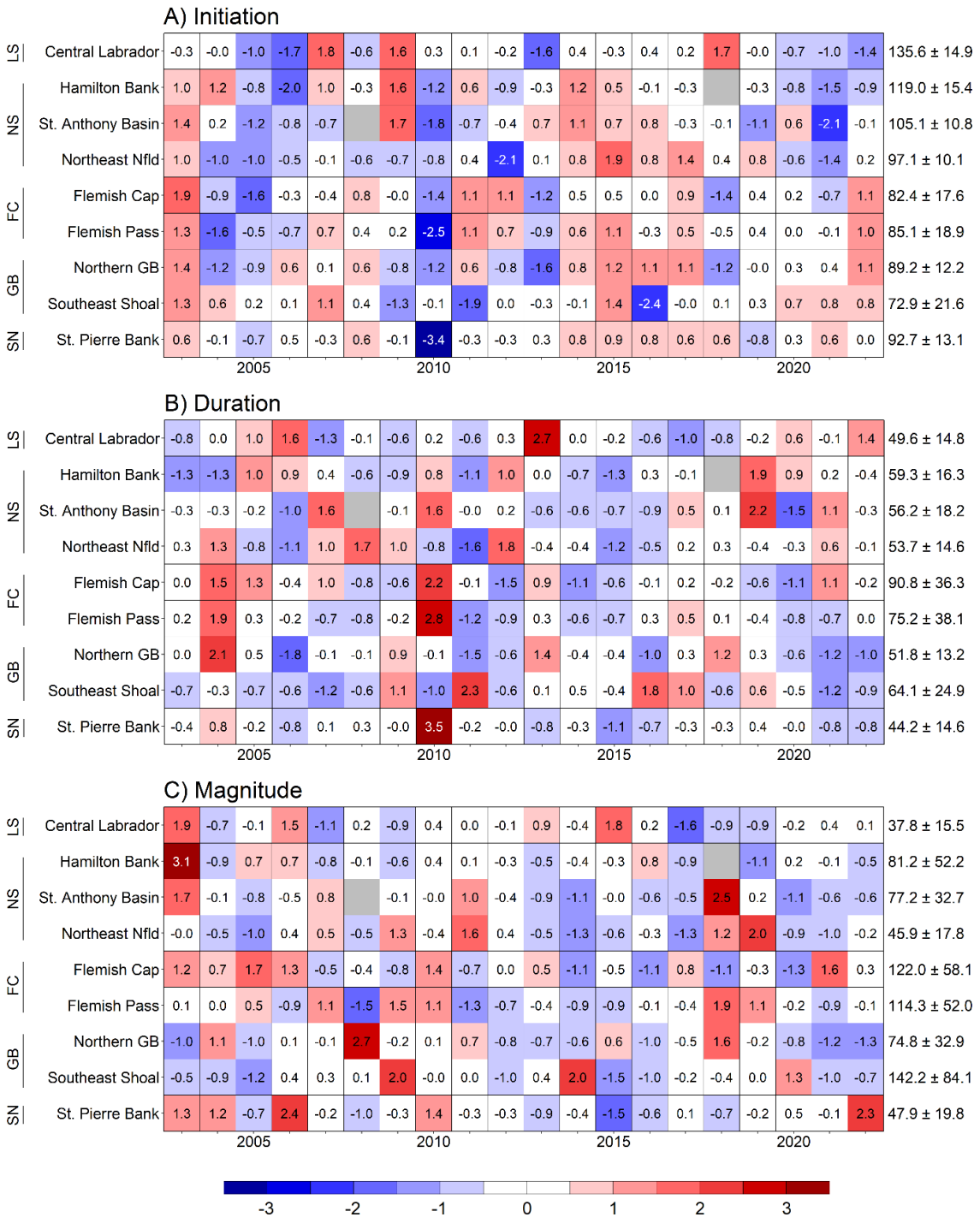

Figure 6. Scorecards of annual anomalies for (A) spring phytoplankton bloom initiation timing, (B) spring bloom duration, and (C) spring bloom magnitude within ocean colour polygons. Numbers in the cells are standardized anomalies based on a 2003-2020 climatology. Climatological means and standard deviations (SD) are listed to the right in units of day of year (initiation), days (duration) and mg of chl a m^{-2} day^{-1} (magnitude). White cells indicate near-normal conditions (±0.5 SD relative to the climatological mean), while blue/red cells indicate earlier/later (initiation), shorter/longer (duration), or lower/higher-than-normal (magnitude) conditions. Polygons are listed from north (top) to south (bottom) on the left and grouped by subregions (EPUs): LS=Labrador Shelf, NS=Newfoundland Shelf, GB=Grand Bank, SN=Southern Newfoundland. See figure 1C for locations of ocean colour polygons and EPUs.

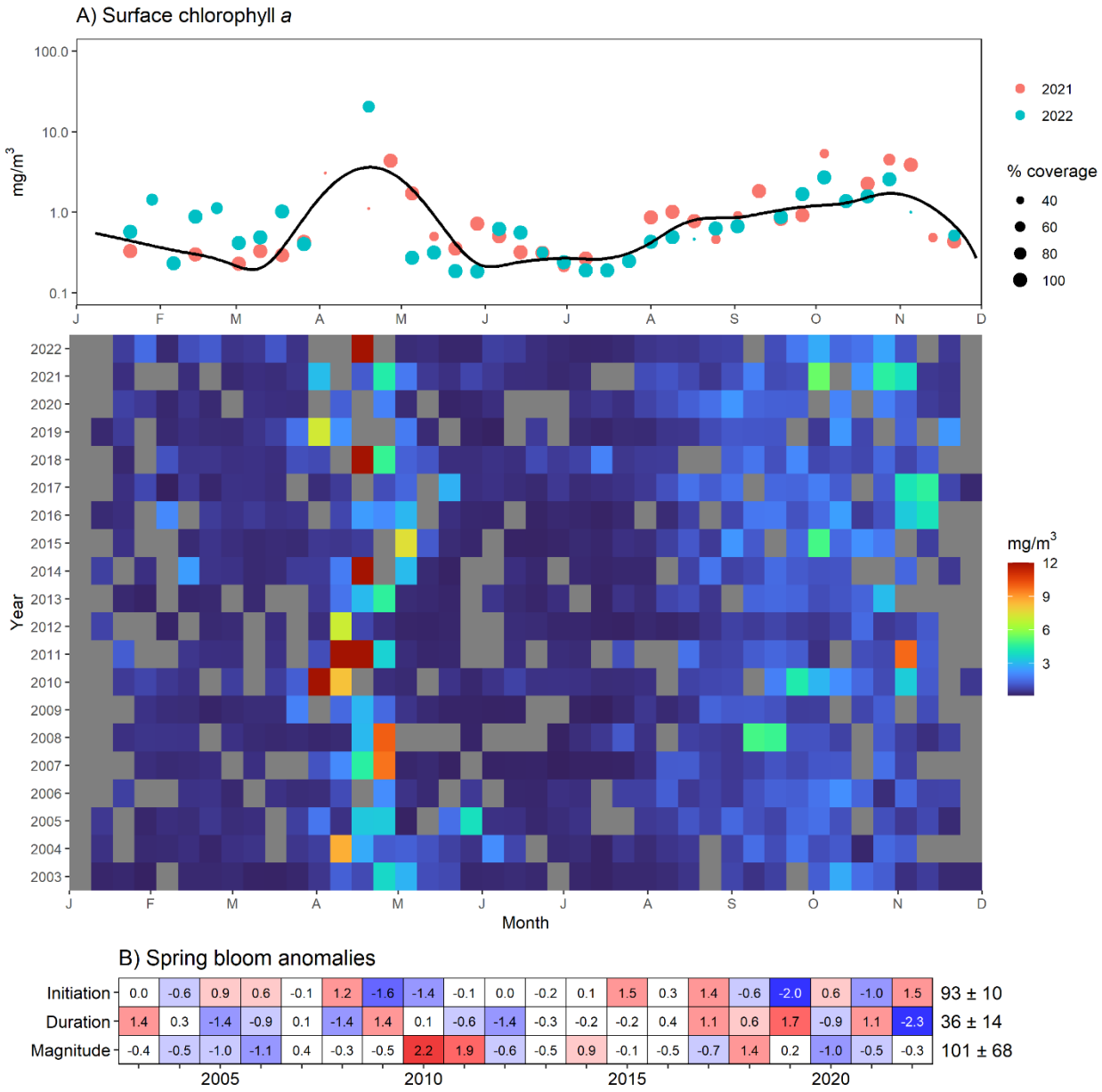

Figure 7. (A) Seasonal variation of 8-day average of surface chlorophyll a (chl a) concentrations detected by satellite observations in a 50-km^2 area around the high-frequency sampling site Station 27 (S27). Black line in the top panel indicates average chl a concentration for the reference period 2003-2020 while dots color and size indicate observation year and satellite percent coverage, respectively. Grey cells in the bottom panel indicate 8-day period during which data was not available. No satellite data were available for December. (B) Scorecards of annual anomalies for spring phytoplankton bloom initiation timing, duration and magnitude at S27. Numbers in the cells represent standardized anomalies based on a 2003-2020 climatology. Climatological means standard deviations (SD) are listed to the right in units of day of year (initiation), days (duration) and mg of chl a m^2 day^{-1}(magnitude). White cells indicate near-normal conditions (±0.5 SD relative to the climatological mean), while blue/red cells indicate conditions earlier/later (initiation), shorter/longer (duration), or lower/higher (magnitude) than normal.

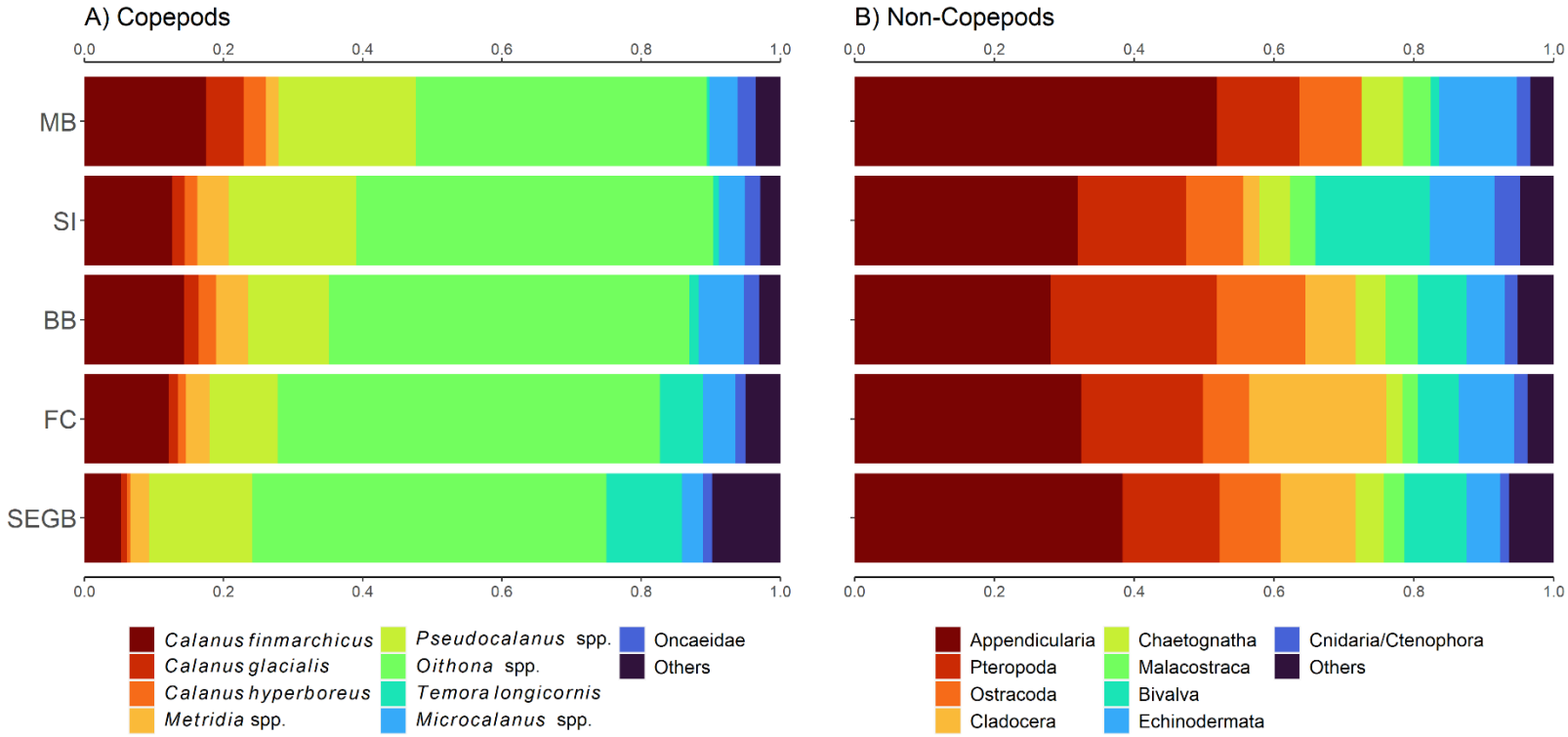

Figure 8. Relative abundance of dominant (A) copepod and (B) non-copepod taxa along AZMP oceanographic sections during the reference period 1999-2020. Sections are listed on the y-axis from north (top) to south (bottom): Makkovik Bank (MB), Seal Island (SI), Bonavista Bay (BB), Flemish Cap (FC), and Southeastern Grand Bank (SEGB). See Fig 1C for location of AZMP sections.

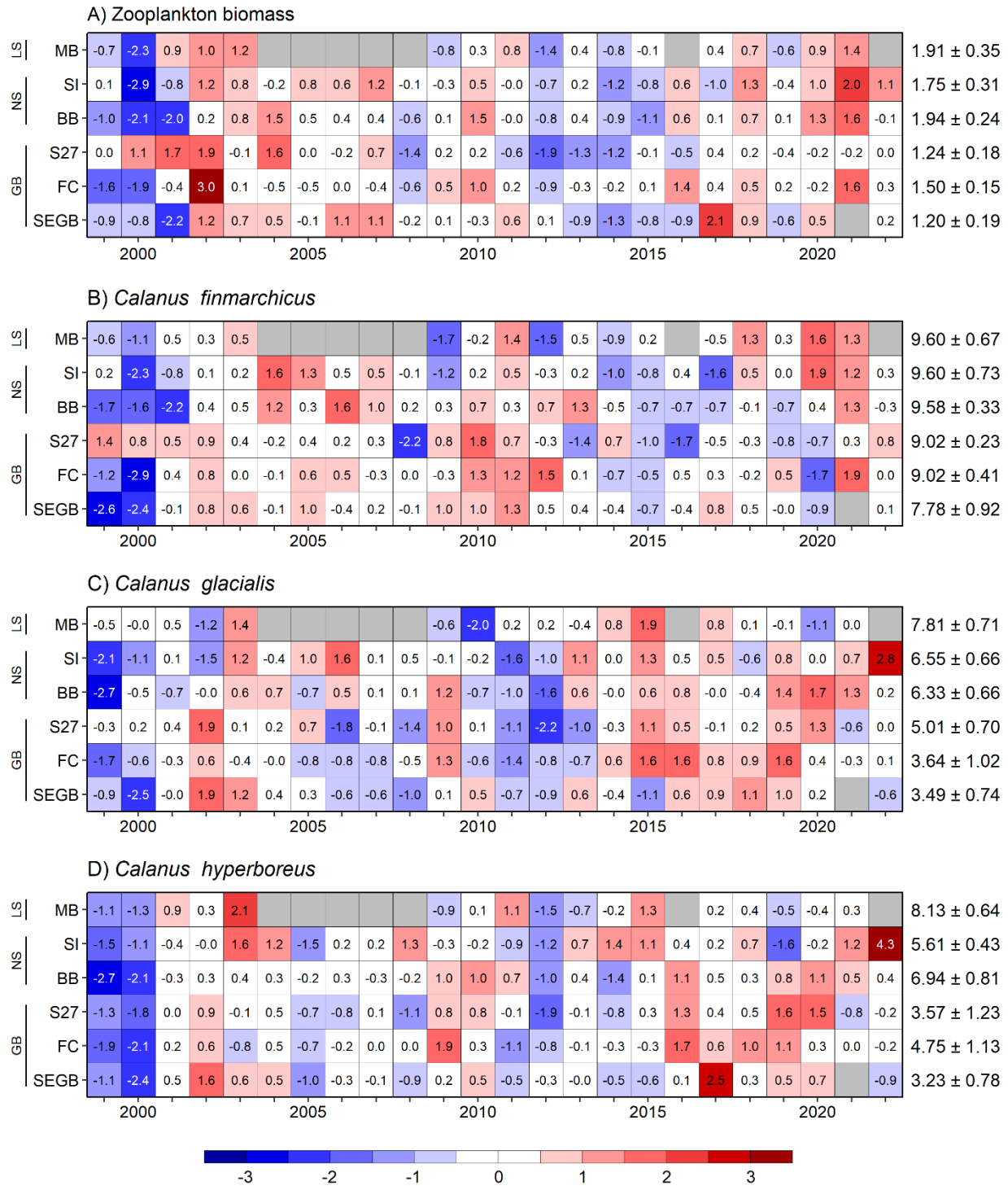

Figure 9. Scorecards of annual anomalies for (A) zooplankton dry biomass, and (B-D) the abundance of the three large Calanus copepod species. Numbers in the cells represent standardized anomalies based on a 1999-2020 climatology. Climatological means and standard deviations (SD) are listed to the right in units of ln(1 + individuals·m^{-2}) for abundance, and ln(1 + grams·m^{-2}) for biomass. White cells indicate near-normal abundance (±0.5 SD relative to the climatological mean), while blue/red cells indicate abundance below/above normal. Grey cells represent missing data. AZMP sections are listed from north (top) to south (bottom) on the left and grouped by subregions (EPUs): LS=Labrador Shelf, NS=Newfoundland Shelf, GB=Grand Bank. See Figure 1B for locations of AZMP sections and EPUs.

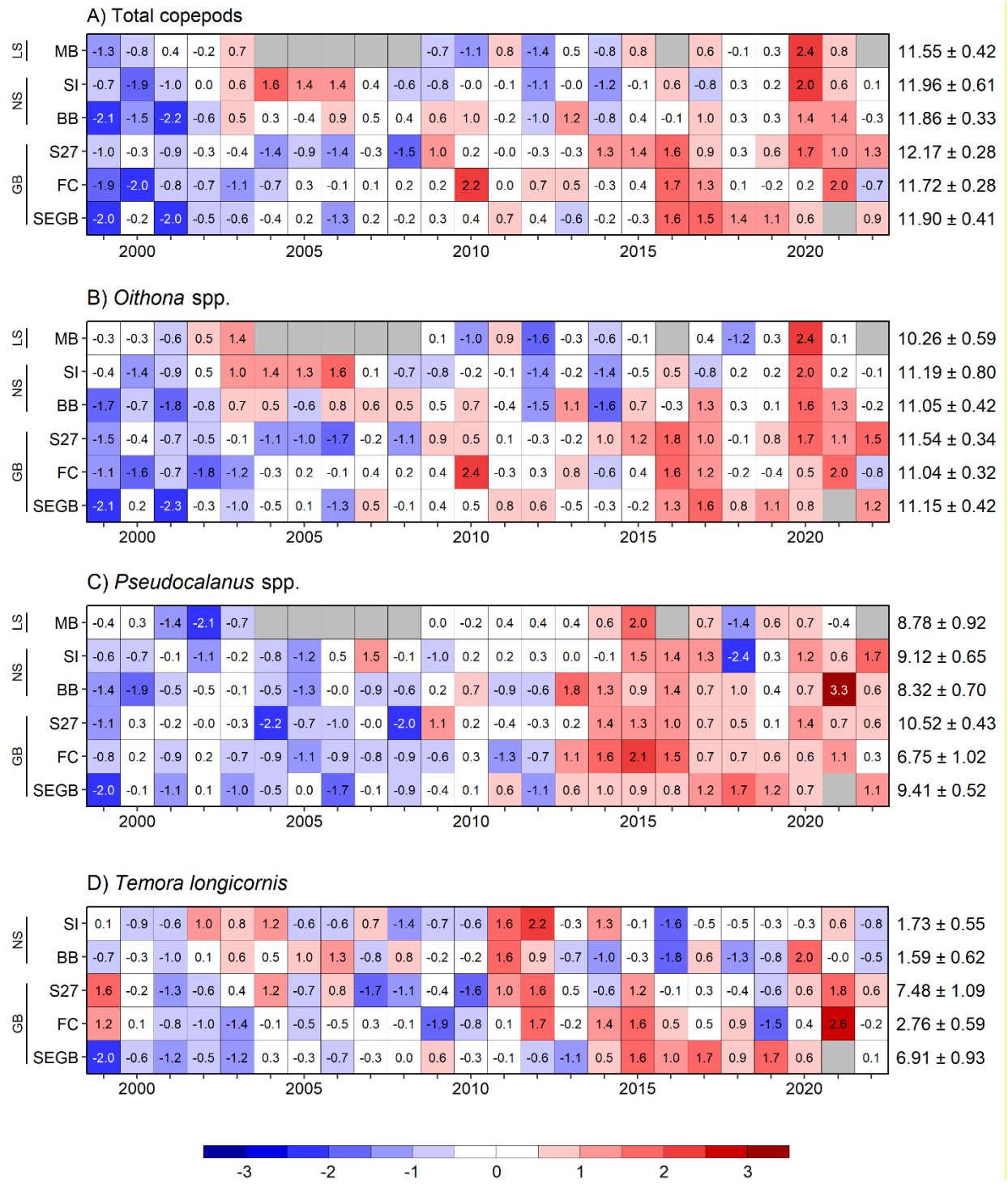

Figure 10. Scorecards of annual anomalies for the abundance of (A) total copepod and (B-D) the three numerically dominant taxa. Numbers in the cells represent standardized anomalies based on a 1999-2020 climatology. Climatological means and standard deviations (SD) are listed to the right in units of ln(1 + individuals·m^{-2}). White cells indicate near-normal abundance (±0.5 SD relative to the climatological mean), while blue/red cells indicate abundance below/above normal. Grey cells represent missing data. AZMP sections are listed from north (top) to south (bottom) on the left and grouped by subregions (EPUs): LS=Labrador Shelf, NS=Newfoundland Shelf, GB=Grand Bank. See Figure 1B for locations of AZMP sections and EPUs.

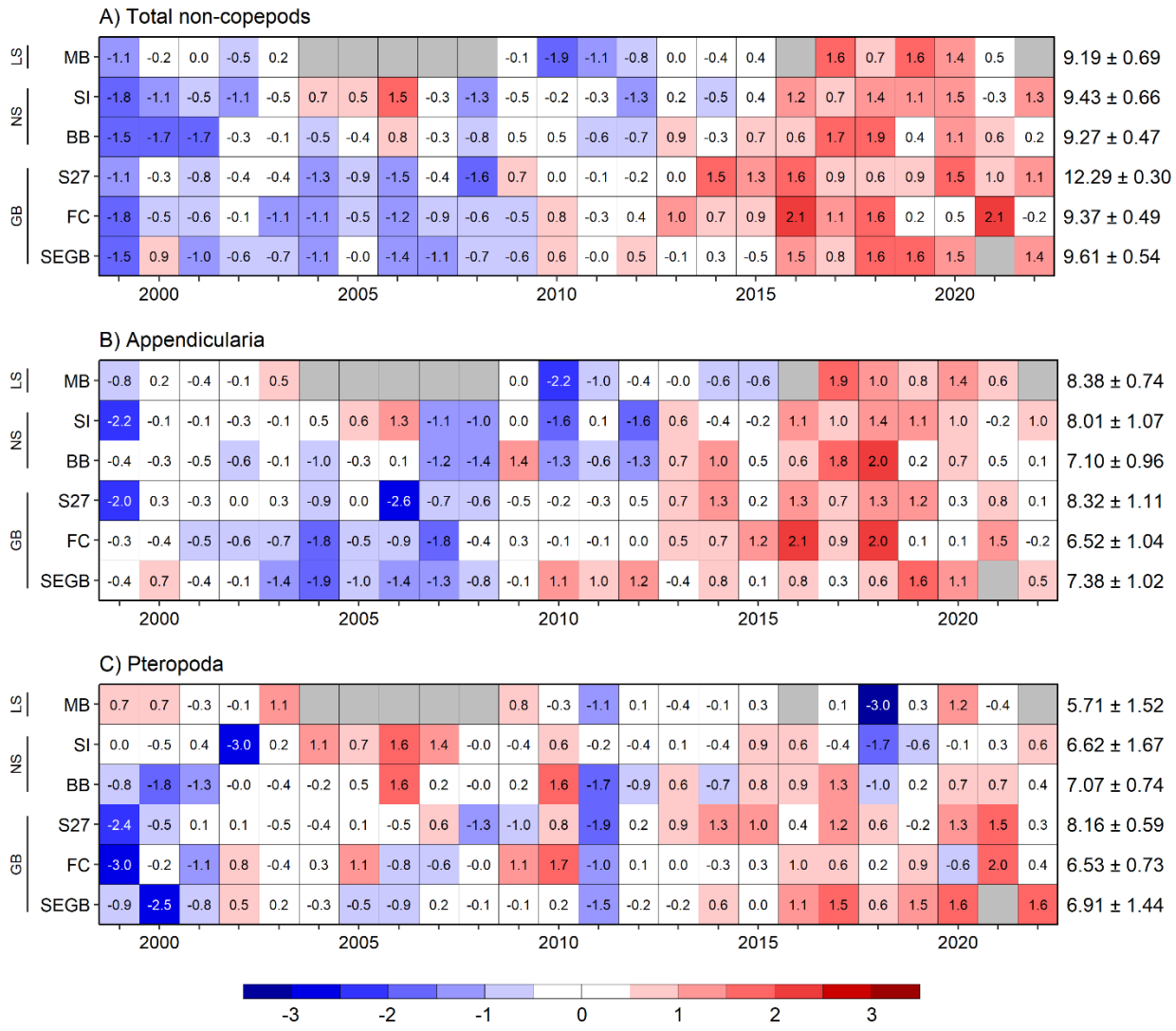

Figure 11. Scorecards of annual anomalies for the abundance of (A) total non-copepods, and (B-C) the two numerically dominant non-copepod taxa. Numbers in the cells represent standardized anomalies based on a 1999-2020 climatology. Climatological means and standard deviations (SD) are listed to the right in units of ln(1 + individuals·m^{-2}). White cells indicate near-normal abundance (±0.5 SD relative to the climatological mean), while blue/red cells indicate abundance below/above normal. Grey cells represent missing data. AZMP sections are listed from north (top) to south (bottom) on the left and grouped by subregions (EPUs): LS=Labrador Shelf, NS=Newfoundland Shelf, GB=Grand Bank. See Figure 1B for locations of AZMP sections and EPUs.

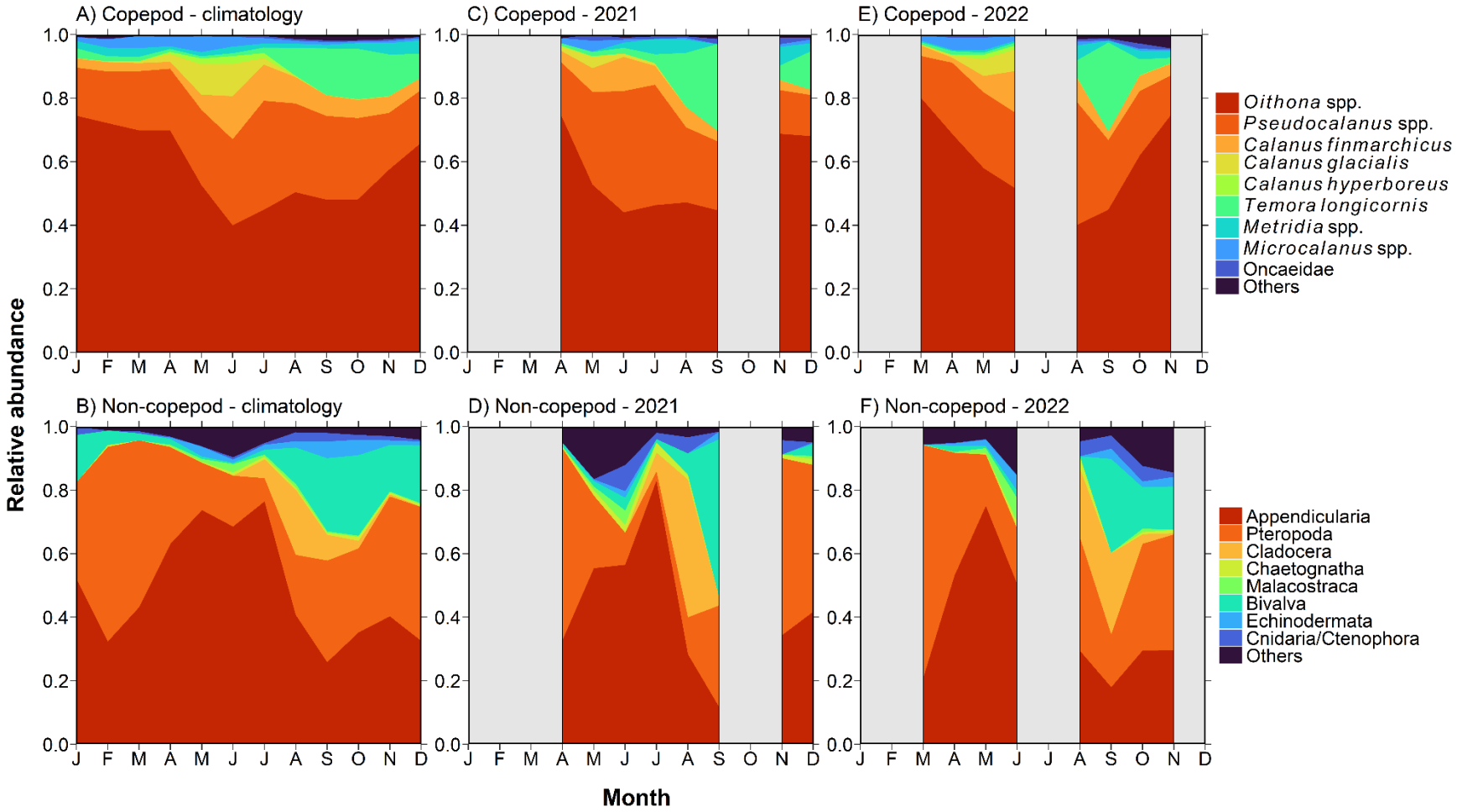

Figure 12. Seasonal variation of copepod (top) and non-copepod (bottom) community composition at Station 27. Climatologies represent average conditions during the 1999-2020 reference period. Data were averaged by month and taxa. Grey areas indicate periods during which no data were available.

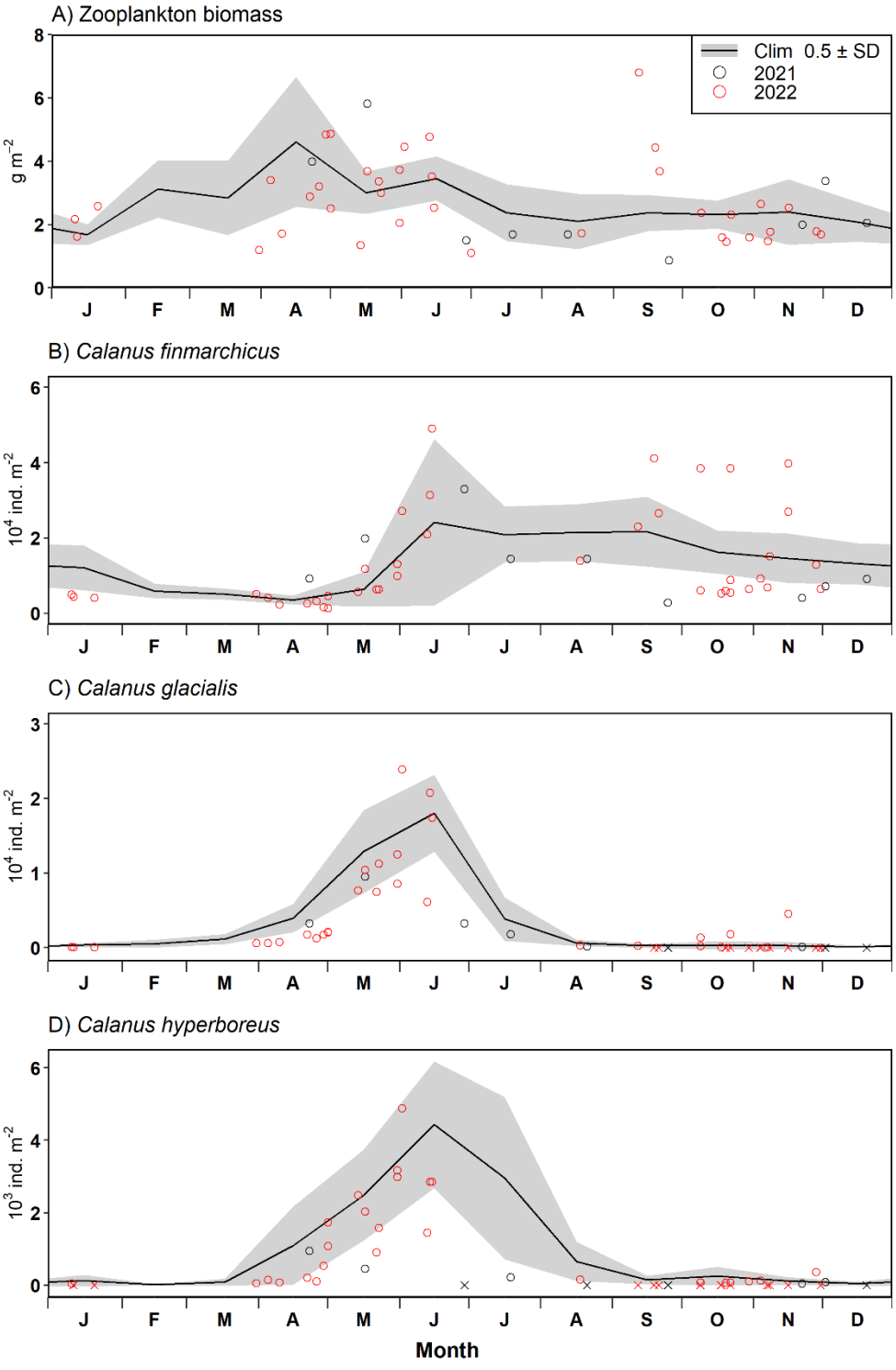

Figure 13. Seasonal cycle of (A) zooplankton dry biomass, and (B-D) abundance of the three large Calanus copepods at Station 27. The black line and grey ribbon represent monthly mean abundance for the reference period 1999-2020. Open circles represent abundances from individual samples. Crosses indicate zero abundance.

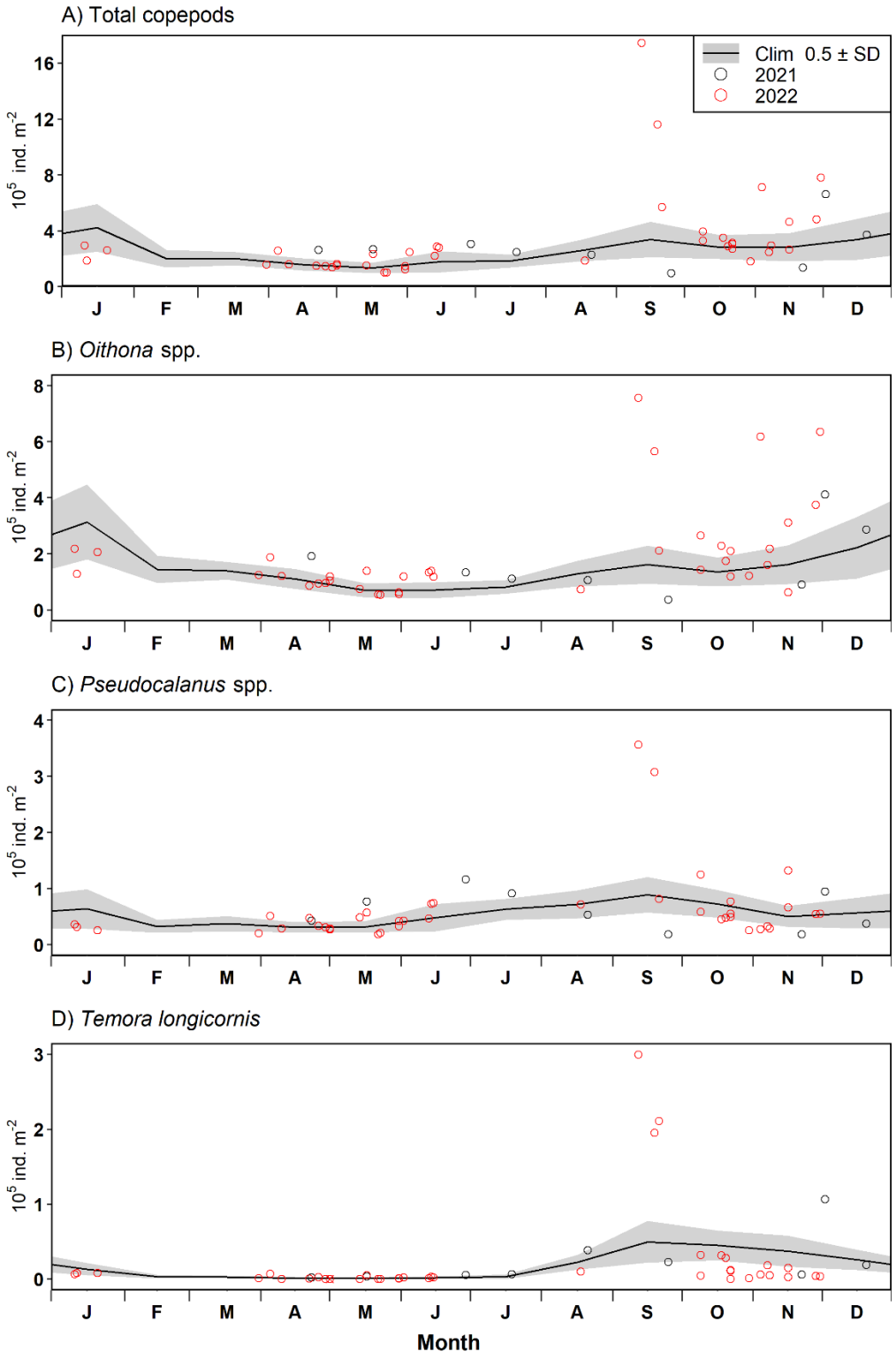

Figure 14. Seasonal cycle of the abundance of (A) total copepods, and (B-D) numerically dominant taxa at Station 27. The black line and grey ribbon represent monthly mean conditions for the reference period 1999-2020. Open circles represent abundances from individual samples.

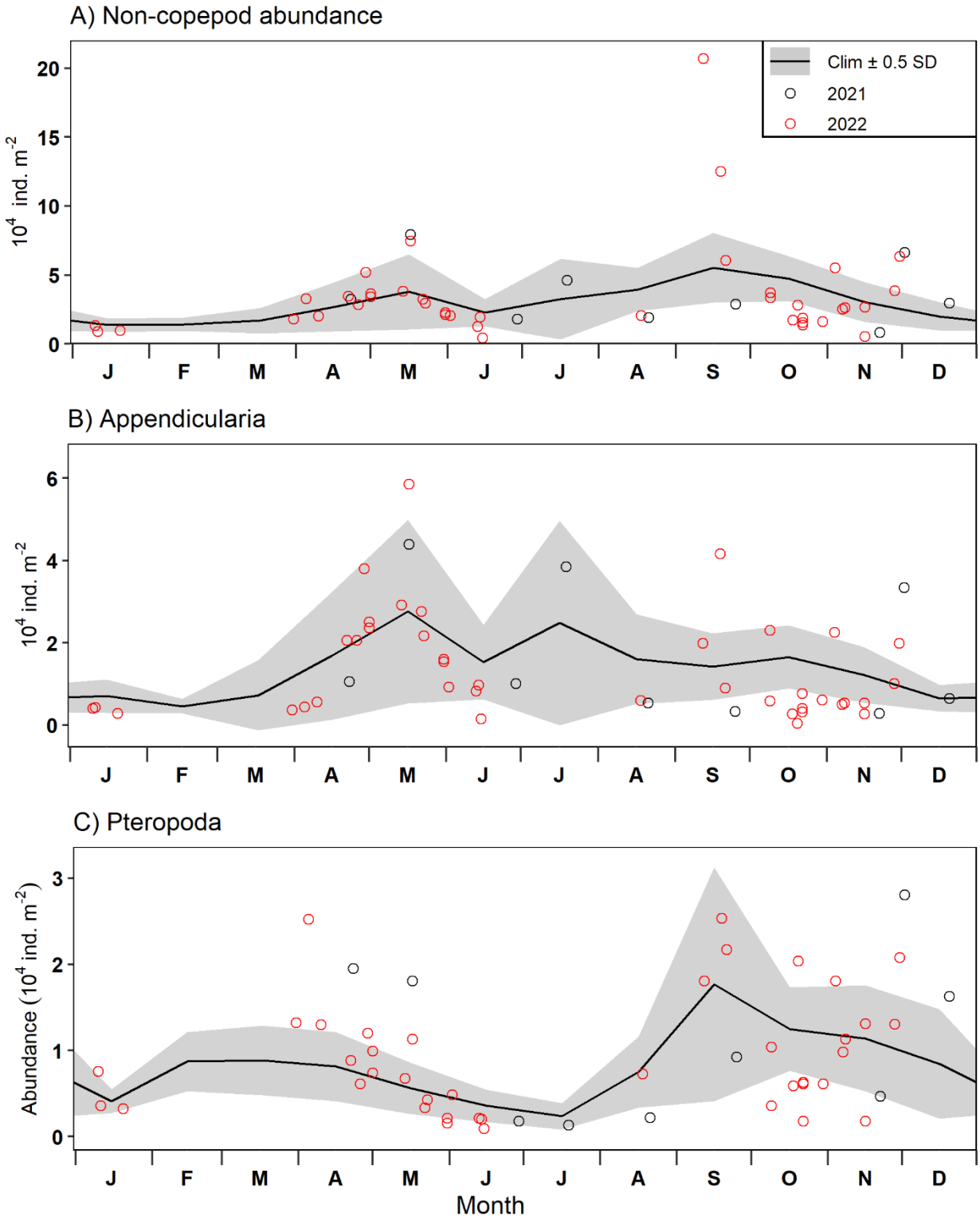

Figure 15. Seasonal cycle in total abundance of (A) total non-copepod organisms and (B-C) the two numerically dominant taxa at Station 27. The black line and grey ribbon represent monthly mean conditions for the reference period 1999-2020. Open circles represent abundances from individual samples.

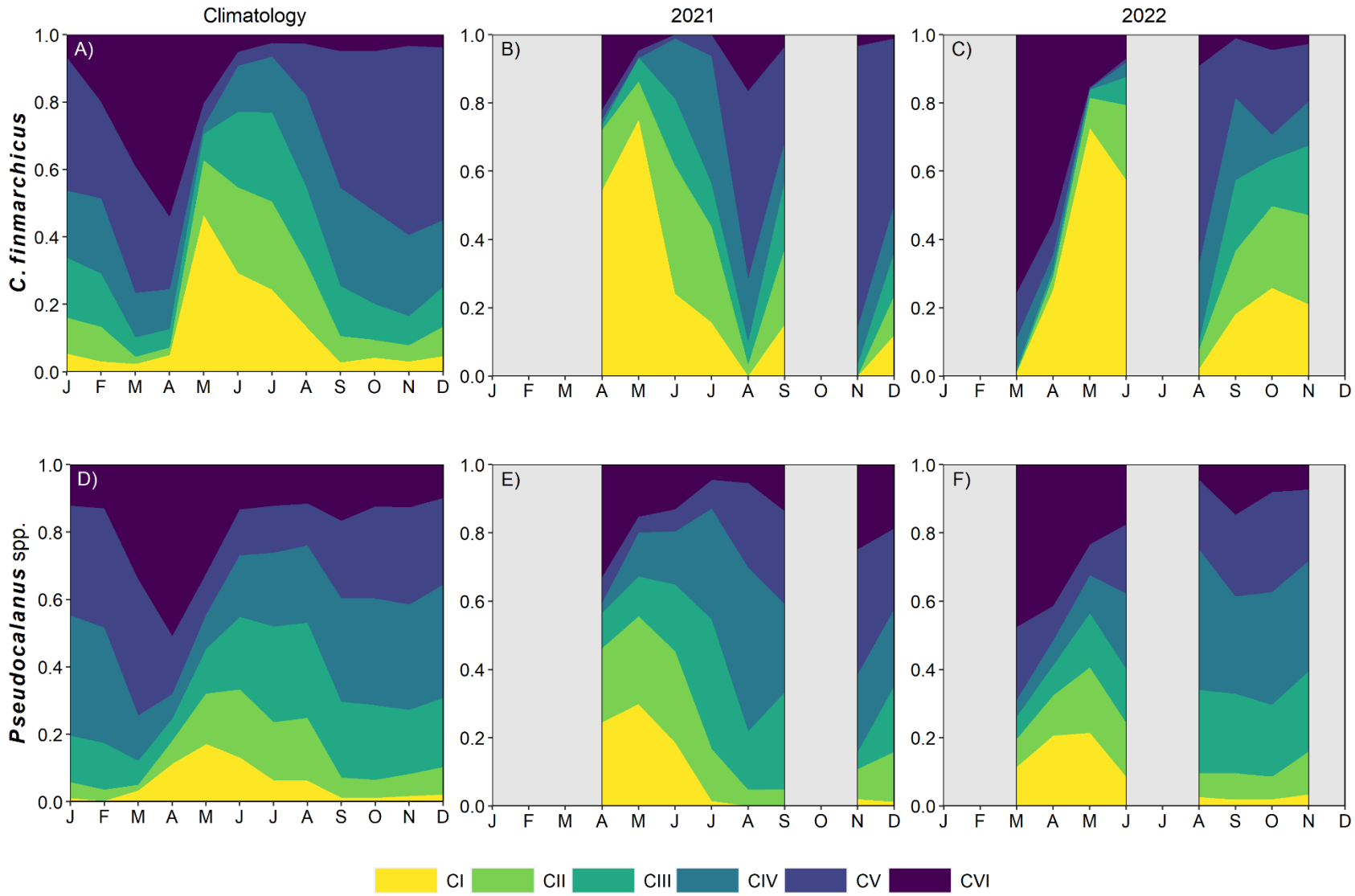

Figure 16. Seasonal cycle in the population structure of Calanus finmarchicus (top) and Pseudocalanus spp. (bottom) copepods at Station 27. Climatologies (left panels) represent average conditions for the 1999-2020 reference period. Data were averaged by month and copepodite stage and are expressed as relative abundances. Grey areas indicate periods during which no data were available.